Tectonophysics 683 (2016) 349–366

Contents lists available at ScienceDirect

Tectonophysics

journal homepage: www.elsevier.com/locate/tecto

Carboniferous granites on the northern margin of Gondwana, Anatolide-Tauride Block, Turkey – Evidence for southward subduction of Paleotethys

O. Candan [a,*], C. Akal [a], O.E. Koralay [a], A.I. Okay [b], R. Oberhänsli [c], D. Prelević [d,e], R. Mertz-Kraus [d]

[a] Dokuz Eylül Üniversitesi, Mühendislik Fakültesi, Jeoloji Mühendisliği Bölümü, Tınaztepe Kampüsü, 35160 Buca, İzmir, Turkey
[b] İstanbul Teknik Universitesi, Avrasya Yer Bilimleri Enstitüsü, 34469 Maslak, İstanbul, Turkey
[c] Institute of Earth and Environmental Sciences, University of Potsdam, Karl Liebknecht Strasse 24, 14476 Potsdam, Germany
[d] Institute of Geosciences, University of Mainz, Becherweg 21, 55099 Mainz, Germany
[e] Faculty of Mining and Geology, University of Belgrade, Djušina 7, 11000 Belgrade, Serbia

ARTICLE INFO

Article history:
Received 28 January 2016
Received in revised form 17 June 2016
Accepted 22 June 2016
Available online 24 June 2016

Keywords:
Carboniferous magmatism
Paleotethys
Gondwana
Afyon zone
Anatolide-Tauride Block

ABSTRACT

Carboniferous metagranites with U-Pb zircon crystallization ages of 331–315 Ma crop out in the Afyon zone in the northern margin of the Anatolide-Tauride Block, which is commonly regarded as part of Gondwana during the Late Palaeozoic. They are peraluminous, calc-alkaline and are characterized by increase in Rb and Ba, decrease in Nb–Ta, and enrichment in Sr and high LILE/HFSE ratios compatible with a continental arc setting. The metagranites intrude a metasedimentary sequence of phyllite, metaquartzite and marble; both the Carboniferous metagranites and metasedimentary rocks are overlain unconformably by Lower Triassic metaconglomerates, metavolcanics and Upper Triassic to Cretaceous recrystallized limestones. The low-grade metamorphism and deformation occurred at the Cretaceous-Tertiary boundary. There is no evidence for Carboniferous deformation and metamorphism in the region. Carboniferous arc-type granites and previously described Carboniferous subduction-accretion complexes on the northern margin of the Anatolide-Tauride Block suggest southward subduction of Paleotethys under Gondwana during the Carboniferous. Considering the Variscan-related arc granites in Pelagonian and Sakarya zones on the active southern margin of Laurasia, a dual subduction of Paleotethys can be envisaged between Early Carboniferous and Late Permian. However, the southward subduction was short-lived and by the Late Permian the Gondwana margin became passive.

1. Introduction

The Cambrian to recent evolution of the Eastern Mediterranean region can be described as successive amalgamation of Gondwana-derived continental blocks to Laurasia (Stampfli et al., 2013 and references therein). This process involved opening of new oceanic basins in the south and closure of old ones in the north (Şengör and Yılmaz, 1981; Okay and Tüysüz, 1999; Stampfli and Borel, 2002). In the eastern Mediterranean, E-W trending Alpine suture zones, İzmir-Ankara-Erzincan Suture Zone (IAES) in the north and Bitlis-Zagros Suture Zone (BZSZ) in the south corresponding to the Northern and Southern branches of the Neotethys, respectively, divide Anatolia into three tectonic units, from north to south as the Pontides, the Anatolides-Taurides and the Arabian Plate (Fig. 1; Ketin, 1966; Okay and Tüysüz, 1999). Contrary to well-documented Neotethyan history, however, the possible location or existence of the Paleotethys suture in Turkey has been the subjects of a long-lasting debate (Stampfli, 2000; Okay, 2000; Göncüoğlu et al., 2003; Topuz et al., 2013).

The Anatolide – Tauride Block is bounded to the north by the İzmir-Ankara-Erzincan suture and to the south by the Bitlis – Zagros suture (Fig. 1). It is generally accepted that until the Late Palaeozoic, the entire present tectonic units in the south of the İzmir – Ankara – Erzincan suture zone, e.g. the Anatolide-Tauride Block and the Arabian Plate, constituted a part of the northern margin of Gondwana, a position close to present-day Arabia (Şengör et al., 1984; Şengör and Yılmaz, 1981; Robertson and Ustaömer, 2009a,b; Linnemann et al., 2009; Torsvik and Cocks, 2013). The Anatolide-Tauride Block became separated from Gondwana during the Triassic by the opening of the southern branch of the Neotethys, and collided with the Pontides during the Early Cenozoic as a consequence of the closure of the Northern branch of Neotethys (Şengör and Yılmaz, 1981; Okay and Tüysüz, 1999). The southern part of the Anatolide-Tauride Block, called as the Taurides, consists of an Infra-Cambrian basement overlain by Cambrian to Eocene

* Corresponding author.
E-mail address: osman.candan@deu.edu.tr (O. Candan).

http://dx.doi.org/10.1016/j.tecto.2016.06.030
0040-1951/

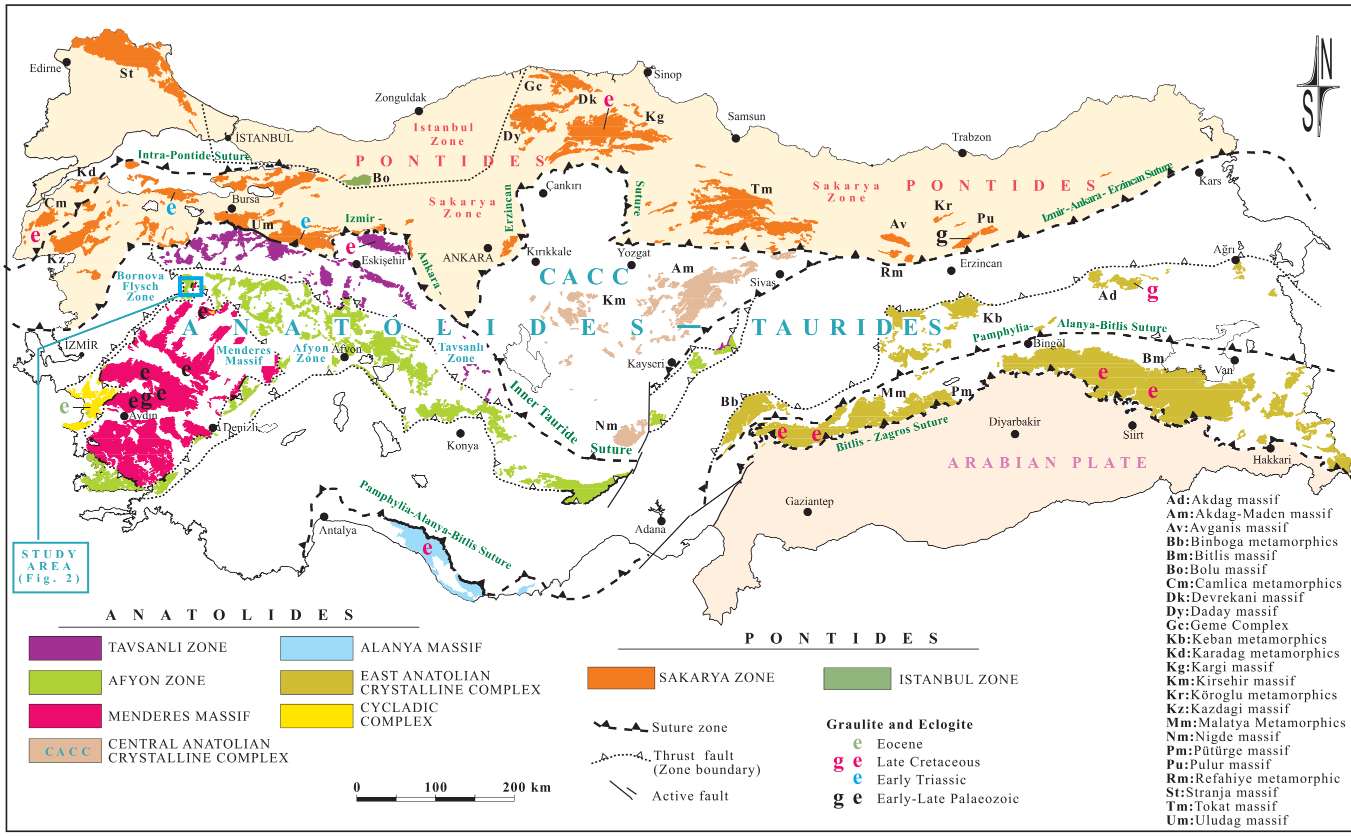

Fig. 1. General distribution of the metamorphic massifs on the tectonic map of Turkey simplified after MTA (2002). The location of the study area is shown by rectangle. This detailed map of Turkey combining the main tectonic lines and the metamorphic areas/zones will be published first time and, most probably, will be used by researches working on metamorphic history of Turkey as a reference map. In this context, we think, if possible, to publish it as a one page may be more useful for the related researchers.

marine sediments (e.g., Özgül, 1984, 1997; Gutnic et al., 1979). However, the Anatolides, which are the metamorphic equivalents of Taurides were involved in the Alpine orogeny and were intensely deformed and metamorphosed during the Late Cretaceous to Early Cenozoic (Fig. 1; Okay et al., 2001; Candan et al., 2005). In the western Anatolia, the northern part of the Anatolide-Tauride Block is subdivided into several tectonic zones, from north to south as Tavşanlı Zone, Afyon zone and Menderes Massif, each characterized by different types and ages of Alpine metamorphism (Fig. 1). The Tavşanlı Zone has undergone HP-LT metamorphism and deformation during the Late Cretaceous (Sherlock et al., ca. 80 Ma), whereas blueschist facies metamorphism in the Afyon zone and Lycian Nappes occurred later at the Cretaceous-Tertiary boundary (Pourteau et al., 2013). The metamorphism in the Menderes Massif is of Barrovian type and took place during the Eocene (Bozkurt and Satır, 2000).

The Pontides in the northern Turkey, consisting of three tectonic units, Strandja Massif, İstanbul Zone and Sakarya zone (Fig.1), represent Gondwana-derived blocks accreted to Laurasia during the Carboniferous (Okay and Nikishin, 2015). Sakarya zone of the Pontides is characterized by a pre-Upper Jurassic basement with complex tectono-thermal history and Upper Jurassic to Cretaceous sedimentary and volcanic cover. Late Triassic (203–215 Ma, Okay and Monié, 1997; Okay et al., 2002) eclogites - blueschist and Jurassic magmatic rocks and associated high-T/low-P metamorphic rocks (*c.* 175–160 Ma; Yılmaz and Boztuğ, 1986; Okay et al., 2014a, b; Okay and Nikishin, 2015; Şen, 2007; Nzegge et al., 2006) documented in the basement series are attributed to episodic northward subduction of the Tethys ocean under the southern margin of Laurasia (Topuz et al., 2013 and references therein). Additionally, Carboniferous to Permian metamorphic rocks and associated magmatic arc plutons occurring as dismembered tectonic slices or autochthon basements under cover series have been well-documented in the Sakarya zone (Okay et al., 2006, 2008; Topuz et al., 2004, 2007; Ustaömer et al., 2012a, b). While in the western parts of Sakarya zone these metamorphic rocks, Kazdağı and Uludağ massifs, were almost completely overprinted by Alpine high-T event, in the central and eastern Pontides, Pulur, Kurtoğlu and Narlık-Karadağ metamorphic rocks preserved their Late Paleozoic tectono-thermal records (Okay et al., 2006, 2008; Topuz et al., 2004, 2007; Ustaömer et al., 2012b). Both the high-grade metamorphism and plutonism are included into Variscan belt, which extends from central Europe to the Caucasus (Okay et al., 2006; von Raumer and Stampfli, 2008; Rolland et al., 2011; Stampfli et al., 2002; Neubauer, 2014; Topuz et al., 2004, 2010; Ustaömer et al., 2012b).

As outlined above, until recently, Carboniferous to Permian tectono-thermal events have been restricted only to the Pontides and were placed to the southern margin of Laurasia. The tectonic setting of the northern continental margin of Gondwana during the late Palaeozoic, however, remains controversial. The main issues are the character of the continental margin (active or passive) and polarity of Paleotethys subduction (northward or southward) (Şengör, 1979; Şengör and Yılmaz, 1981; Şengör et al., 1980; Göncüoğlu et al., 2003, 2007; Stampfli and Borel, 2002; Stampfli et al., 2002, 2013; Okay et al., 2006; Robertson and Ustaömer, 2009a, b).

In this study we report widespread Early to mid-Carboniferous metagranites from the Afyon zone in the northern margin of the Anatolide-Tauride Block with the implication of Carboniferous plutonism on the northern margin of Gondwana. We obtained reliable geochronological, geochemical and stratigraphic data from these newly discovered Carboniferous granite bodies and associated host-rocks in the Afyon zone of the Anatolides (Akal et al., 2011a; Hasözbek et al., 2011). Because the Afyon zone displays a Gondwanan affinity, these data are critically important to unravel the perplexing Late

Palaeozoic tectonic evolution of northern margin of Gondwana. Furthermore, we compare these granites with the Carboniferous to Permian magmatic activity assigned to the Variscan orogeny along the southern margin of Laurasia from central Europe to the Caucasus and suggest that Afyon zone granites are unrelated to the Variscan event. Finally, we suggest a tectonic model for the Late Palaeozoic evolution of the northern margin of Gondwana, which starts with southward subduction beneath the Gondwana and ends with the establishment of a passive continental margin setting.

2. Geological framework

2.1. Afyon zone

The Afyon zone, one of the tectonic zones of the Anatolide-Tauride Block, extends east-west for >600 km and is made up of Latest Neoproterozoic to Late Cretaceous units (Göncüoğlu et al., 2007; Candan et al., 2005; Pourteau et al., 2013; Özer and Özgen, 2012). Three distinct pre-Mesozoic basement lithologies, which are unconformably covered by a common Early Triassic to Late Cretaceous coherent series, have been recognized. The first type is sillimanite-bearing Late Neoproterozoic schists with a poly-phase deformation and metamorphism, which are intruded by Precambrian (*c.* 550 Ma) gabbros and granites (Özcan et al., 1988; Candan et al., 2005; Gürsu et al., 2004). The high-grade metamorphism is attributed to the final amalgamation stage of Gondwana during the Neoproterozoic Pan-African orogeny (Candan et al., 2005). The second type consists of pre-Carboniferous schist and marble intercalation and is only documented at the northwestern edge of the Afyon zone, around Simav area. It is probably Infra-Cambrian in depositional age, and is characterized by numerous Carboniferous granitoid intrusions (Hasözbek et al., 2011; Akal et al., 2011a). The third type of basement is composed of an intercalation of metaquartzite, schist and black marble. Based on the fossils, a Carboniferous to Upper Permian age is inferred for this series, which constitutes the metamorphic equivalents of Upper Palaeozoic nonmetamorphic Tauride series (Özcan et al., 1988; Göncüoğlu et al., 2007). The major unconformity between the basement units and Early Triassic to Late Cretaceous coherent cover series represents a deep subaerial erosion. The overlying Triassic series start with continental coarse-grained metaclastics and associated metavolcanics of metarhyolite, metarhyodacite and metatrachyandesite (Eren et al., 2004; Candan et al., 2005; Robertson and Ustaömer, 2009b, 2011; Akal et al., 2012). The metavolcanics have yielded Early to Middle Triassic U-Pb zircon ages clustering at about 250–230 Ma (Akal et al., 2012; Özdamar et al., 2013), and pass upward into reddish phyllites, which are overlain by platform-type thick Upper Triassic to Upper Cretaceous carbonates and Campanian metaolistostromes (Özcan et al., 1988; Göncüoğlu et al., 2007; Özer and Özgen, 2012). The regional metamorphism is in blueschist to greenschist facies and has occurred at the Cretaceous-Tertiary boundary (Candan et al., 2005; Pourteau et al., 2013).

2.2. Geology of Simav area

Simav area, located close to the northwestern edge of the Afyon zone, displays a tectonic stack (Figs. 2b–3). The main tectonic units are, from the base upwards, *i*) a metamorphosed ophiolitic mélange, *ii*) high-grade rocks of the Menderes massif, *iii*) low-grade units of the Afyon zone and *iv*) non-metamorphic Upper Cretaceous ophiolitic mélange (Bornova Flysch Zone). This tectonic stack is cross-cut by Oligo-Miocene syn-extensional granites and is covered by Early Miocene continental sedimentary and volcanic rocks (Fig. 3).

The lowermost tectonic unit, metamorphosed ophiolitic mélange, is made up of predominantly metamorphic serpentinites with minor amount of amphibolite, amphibolitic metagabbro and marble blocks with medium-pressure mineral assemblages. In Western Anatolia, metamorphosed ophiolitic mélange occurs in two tectonic units: Cycladic Complex and Tavşanlı Zone. Both units are characterized by well-preserved blueschist - eclogite facies metamorphism (Candan et al., 1997; Okay, 2002). Furthermore, Cycladic Complex occurs as a tectonic unit sandwiched between overlying Afyon zone-Lycian Nappes and underlying Menderes Massif (Ring et al., 1999). Similarly, Tavşanlı Zone, which is tectonically underlain by the Afyon zone, doesn't have a contact with the Menderes Massif. Considering these geological constrains, correlation of this metamorphosed ophiolitic mélange with the main tectonic units of the Western Anatolia remains unknown.

The metamorphosed ophiolitic mélange is tectonically overlain by partly migmatized sillimanite-bearing homogenous paragneisses. They are fine-grained, massive to weakly foliated reddish to violet rocks, which can be correlated with the Latest Neoproterozoic paragneiss unit forming the dominant lithology of the Precambrian basement of the Menderes massif (Dora et al., 2001).

The third tectonic unit is made up of a basement, probably of Infra-Cambrian age, and unconformably overlying Lower Triassic and younger volcanosedimentary cover sequence of the Afyon zone. The basement consists of phyllite-quartz schist intercalation with marble lenses up to 2 km in length. They are intruded by numerous Carboniferous granite bodies with various sizes ranging up to 4 km in length and their aplitic vein rocks (Fig. 2b). The metaclastic rocks and the Carboniferous metagranites are unconformably overlain by metaconglomerates reaching up to 500 m in thickness. They consist of quartzite clasts ranging in size from cobble to gravel in a quartz-rich sandy matrix. The metaconglomerates are interbedded with fine grained metaquartzite, quartz phyllite and rarely with thin carbonate horizons. Towards the upper levels they pass or interfinger gradually with metavolcanic rocks. The metavolcanic sequence, up to 250–300 m in thicknesses, is predominantly made up of metamorphosed rhyolitic, rhyodacitic and dacitic lava flows and associated epiclastics/pyroclastics volcanic rocks. U-Pb zircon dating from the metavolcanic rocks yields Middle Triassic ages (240–243 Ma, Akal et al., 2012), implying an Early Triassic age for the underlying basal metaconglomerates. Non-metamorphic Late Cretaceous mélange (Bornova Flysch Zone), composed of basalt, radiolarian chert, pelagic/neritic limestone and serpentinite, constitutes the uppermost tectonic unit.

3. Petrography of the Carboniferous metagranites

Carboniferous granites form the dominant lithology of the pre-Triassic basement of the Afyon zone in the Simav area, constituting over 60% of the basement (Fig. 2b). Sixteen individual bodies showing intrusive contact relationship with low-grade country rocks have been distinguished. According to their primary textures, two types of metagranites can be described: *i*) medium-grained granoblastic metagranite and *ii*) coarse-grained porphyritic metagranite. In some places they intrude into each other. The contacts between two types of granites are sharp; however, the relative age relation among these intrusions cannot be established in the field.

3.1. Granoblastic metagranites

Granoblastic metagranites are medium-grained (0.5–1 cm) rocks that can easily be distinguished by their typical grayish to white color. In the field, they are characterized by a variable mylonitic texture, pronounced foliation and a NNE-trending lineation defined by parallel alignment of recrystallized feldspar aggregates. The penetrative Alpine foliation is defined by quartz ribbons and development of metamorphic white mica and chlorite (Fig. 4b). However, the primary equigranular granoblastic texture of the granite can still be recognized in low-strain domains (Fig. 4a). Intrusive contact relationship with the country rocks can be observed 1 km east of the village Karacalar (Fig. 4c). The widespread aplitic veins along the granite contact in both country rocks and granite themselves, schist enclaves in the granites as well as

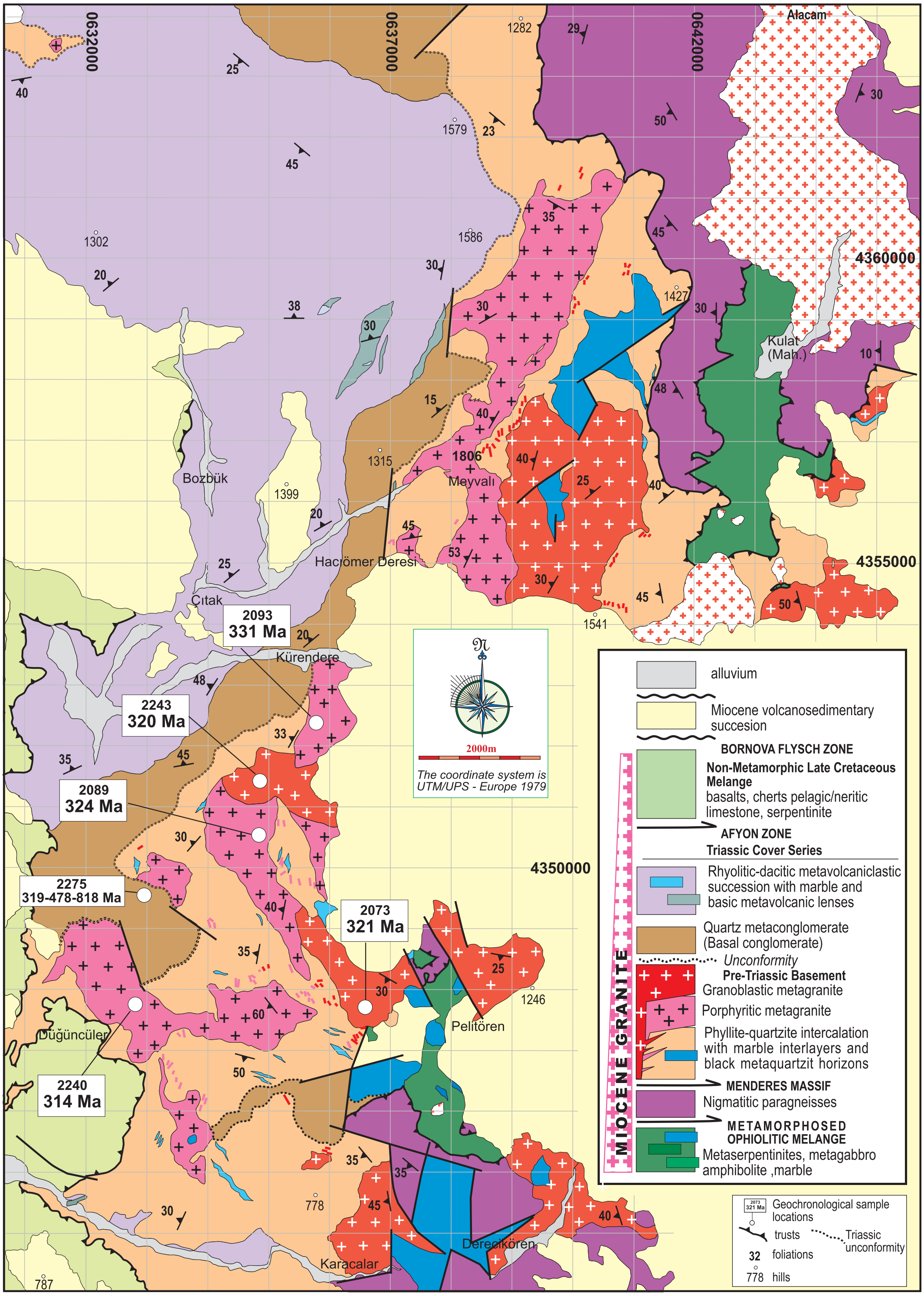

Fig. 2. Detailed geological map of the Simav area located at the northwestern part of the Afyon zone.

rare contact metamorphic effects in carbonate-rich schists attest to the original intrusive character of the metagranites. The mylonitic foliation of the metagranites shows close parallelism with the regional foliation of the country rocks and with the foliation of the overlying Triassic sequence favoring a common single-stage regional deformation during Alpine metamorphism.

The mineral assemblage of the granoblastic metagranites is K-feldspar (48–44 vol.%), plagioclase (19–23 vol.%), quartz (16–22 vol.%), muscovite (8–16 vol.%), chlorite (4–6 vol.%), epidote (2–4 vol.%) with apatite, sphene and zircon as accessory minerals.

3.2. Porphyritic metagranites

Coarse-grained porphyritic metagranites can be distinguished from the granoblastic metagranites by their porphyritic texture and typical greenish color resulting from late chlorite and epidote occurring along

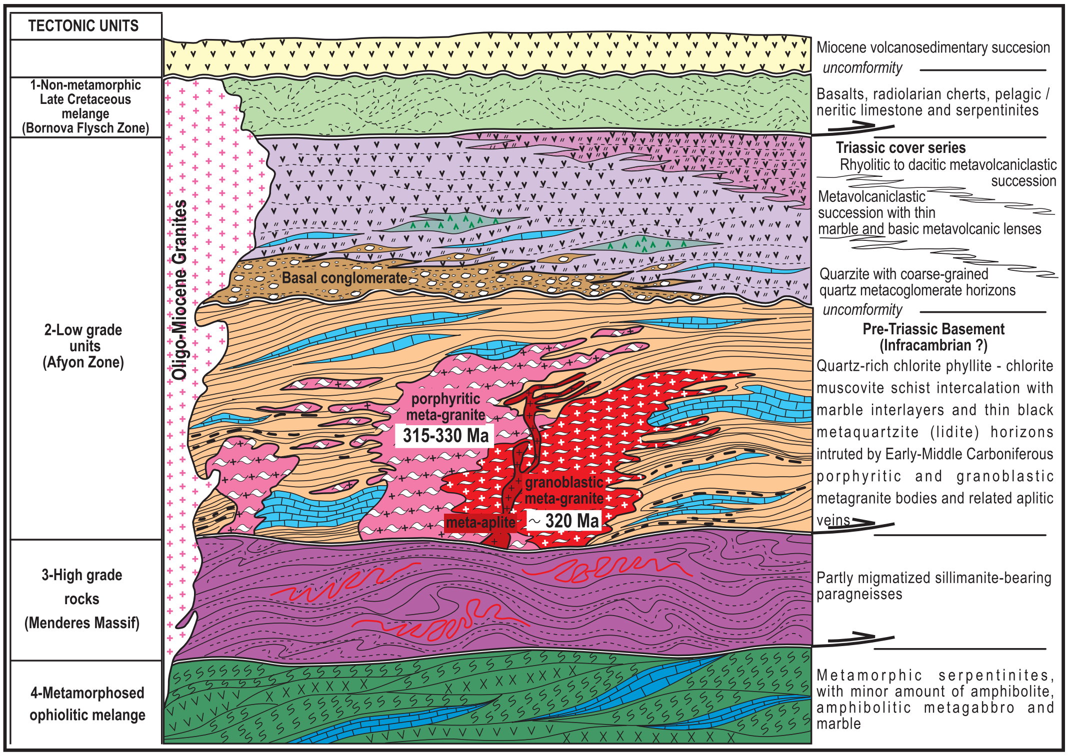

Fig. 3. The generalized tectonostratigraphy of the Simav area. Pre-Triassic basement of the Afyon zone is intruded by Early to Middle Carboniferous granites.

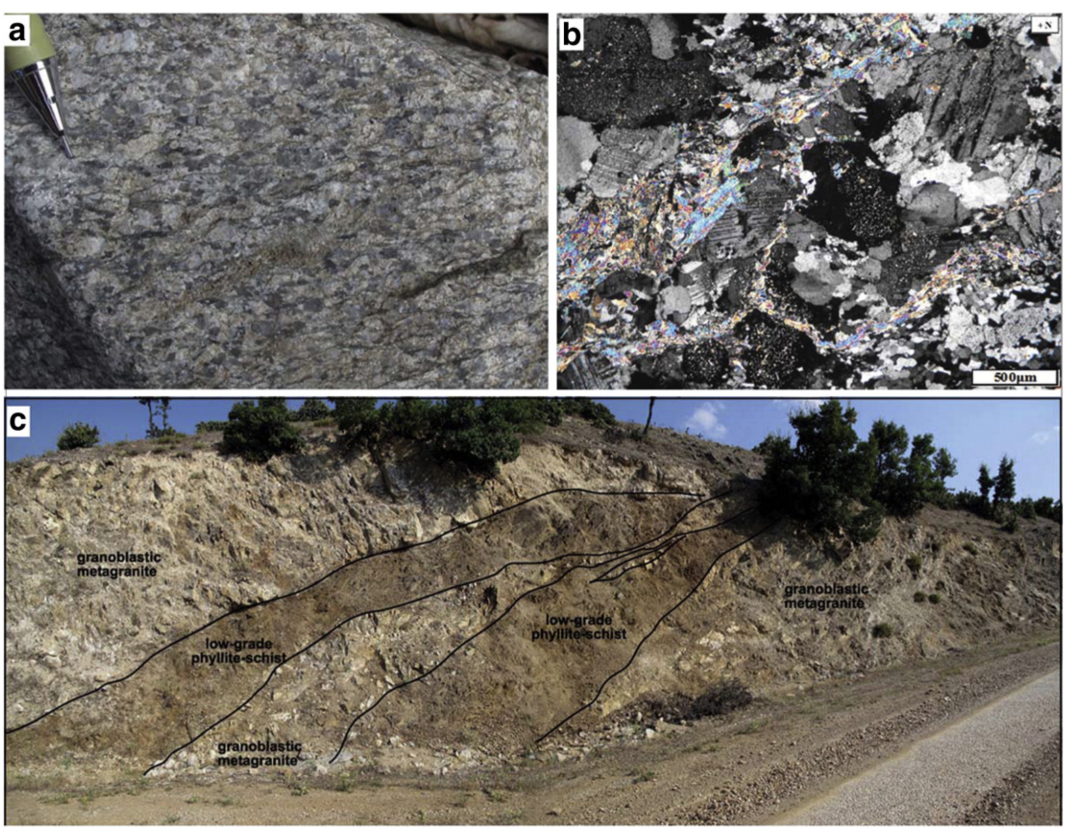

Fig. 4. a) Preserved primary igneous texture modified by ductile shear zones in granoblastic metagranites, b) photomicrograph of ductile deformed granoblastic metagranite. Mylonitic foliation is defined by parallel alignment of white mica-rich cleavage domains and c) well-preserved intrusive contact relationships of the granoblastic metagranites with low-grade phyllite-quartzite-marble series, east of Karacalar village.

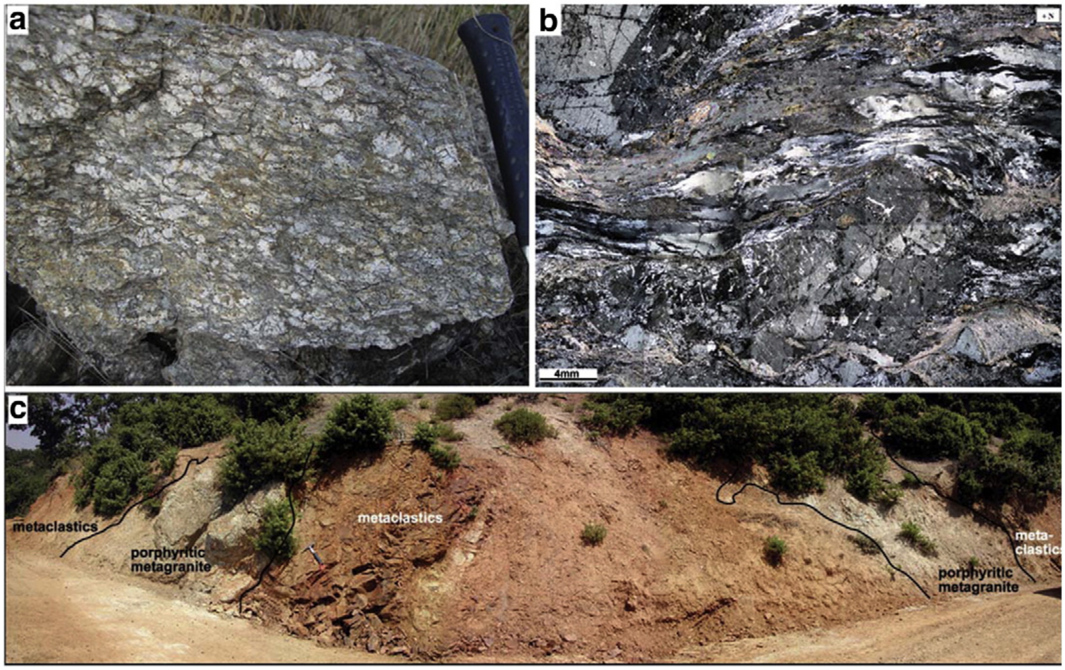

Fig. 5. a) Coarse-grained porphyritic metagranite with blastomylonitic texture, b) photomicrograph of porphyritic metagranite. Mylonitic foliation is defined by quartz ribbons and cleavage domains consisting of predominantly white mica and chlorite with minor epidote crystals and c) preserved intrusive contact relationship between porphyritic metagranite and phyllitic country rocks, north of Meyvalı.

the mylonitic foliation (Fig. 5a). The deformation in the porphyritic metagranites is heterogeneous, and where deformation is not intense, the primary porphyritic texture defined by randomly oriented euhedral to subhedral large orthoclase crystals in a matrix consisting of equigranular medium-grained quartz and feldspar can be readily identified. However, in general, they display a regional blastomylonitic texture with large retort-shape porphyroblasts or augen of K-feldspar, reaching up to 4 cm in length, around which a more ductile, medium- to fine-grained matrix of muscovite, quartz and feldspar is deflected.

The contact between the metaclastic rocks and porphyritic metagranite bodies is best observed 1 km east of Düğüncüler town and Meyvalı village along the road cut (Fig. 5c). Contact is sharp and numerous enclaves of the country rock reaching up to 5 m in size occur as partly assimilated bodies in the granite. Furthermore, within a zone of 50 m around the granite, sills of porphyritic metagranites up to 1 m in thicknesses are observed in the country rocks. In many places, the country rock has become more massive and rich in tremolite/actinolite, epidote and albite towards the granite contacts, which can be attributed to the contact metamorphic effects.

The mineral assemblage of the porphyritic metagranites is K-feldspar (44–48 vol.%), plagioclase (14–18 vol.%), quartz (18–22 vol.%), muscovite (9–12 vol.%), chlorite (4–6 vol.%), epidote (2–3 vol.%) with apatite, sphene and zircon as accessory minerals. In K-feldspar porphyroclasts, typical core-and-mantle structure characterized by a larger core surrounded by a mantle of fine recrystallized grains is very common. The boundaries of adjacent feldspar grains are highly serrated indicating dynamic recrystallization. Recrystallization occurred also along narrow bands crossing porphyroclasts. They show perthitic structure and, especially in highly deformed porphyroclasts, well-developed pericline twinning is common. Undulose extinction, deformation twins and deformation bands are frequent in plagioclase crystals. Quartz exhibits undulose extinction, deformation bands and sub-grain formation. Along the shear zones primary quartz crystals were recrystallized as quartz ribbons (Fig. 5b). In addition to the quartz ribbons, the main foliation of the metagranites is defined by the preferred orientation of the muscovite and chlorite. Muscovites occur as fine-grained crystals interlayered by chlorites. Fine-grained epidotes occur preferentially in mica-rich domains.

4. Geochemistry of the metagranites

Twenty-four representative samples from both types of the metagranites are analyzed for their geochemistry (cf. Table 1 in Supplementary material 2). Analytical methods for sample preparing and whole rock geochemistry are described in Supplementary material 1. All the metagranite samples exhibit relatively high contents of SiO_2 (70.1–77.6 wt%), Al_2O_3 (12.3–15.7 wt%), $Na_2O + K_2O$ (6.1–8.7 wt%) and K_2O (2.1–5.9 wt%) and low contents of CaO (0.1–1.5 wt%), TiO_2 (0.1–0.4 wt%), P_2O_5 (0.01–0.16 wt%) and MgO (0.19–1.47 wt%). In the TAS diagram of Cox et al. (1979), all samples fall in the sub-alkaline granite field (Fig. 6a). A/CNK ratios of metagranites range from 1.1 to 1.6 and plot in the peraluminous field of Maniar and Piccoli (1989) (Fig. 6b). In the K_2O versus SiO_2 diagram, porphyritic metagranites plot in the high-potassic calk-alkaline field, while granoblastic metagranites are scattered in the medium- and high-K calk-alkaline fields according to the classification scheme suggested by Le Maitre (2002) (Fig. 6c). All metagranites exhibit a typical calc-alkaline trend on AFM diagram of Irvine and Baragar (1971) (Fig. 6d).

Primitive mantle-normalized incompatible element abundance of both types of the metagranites display similar patterns characterized by positive anomalies of Rb, Ba, Th, U, K and negative anomalies of Nb-Ti, Y and P (Fig. 7a). Increase of Rb and Ba together with decrease of immobile elements such as Nb–Ta, and enrichment of Sr are inferred as the indicators of subduction-related processes in active continental margins (Sun and McDonough, 1989). The high LILE/HFSE ratios of the Carboniferous granites also indicate subduction zone magmatism and over-thickened crust, which may be related to the tectonic history of active continental margins (Saunders and Tarney, 1980; Bailey, 1981).

The total REE contents of all the samples are relatively high (up to 295 μg/g). The C1-chondrite-normalized REE distribution patterns of

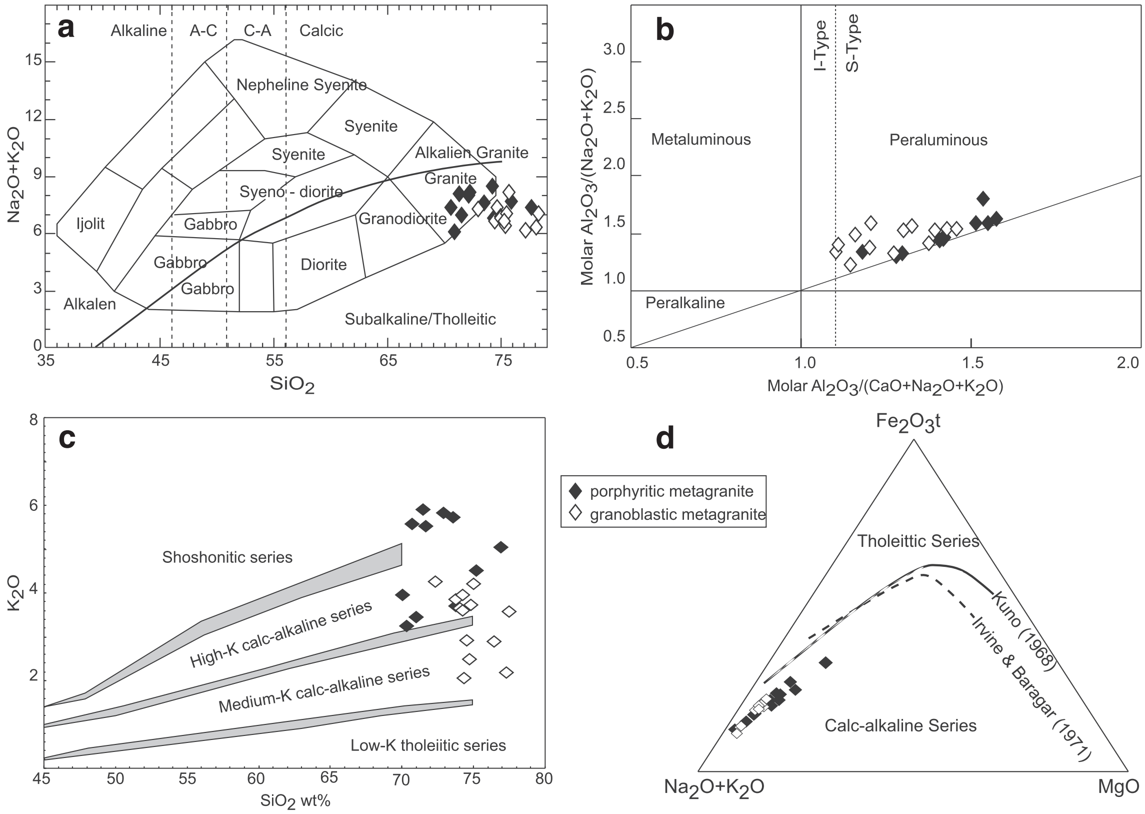

Fig. 6. a) Total alkalis versus SiO2 (wt.%) diagram, b) plot of the A/CNK ratios, c) compositional characteristics of metagranites on K2O vs. SiO2 diagram after Le Maitre (2002) showing high- to ultrahigh-K composition and d) calc-alkaline trend of the metagranites on the AFM diagram (Irvine and Baragar, 1971).

all samples exhibit the enrichment of LREEs and relative to depletion in HREEs, indicating weak fractionation [$(Gd/Yb)_{CN} = 0.8–4.7$] (Fig. 7b). Slight but consistent negative Eu ($Eu/Eu^* = 0.28–0.89$) and Sr anomalies suggest fractionation of the plagioclase in the source during magma crystallization (Wilson, 1989). The weakly fractionated HREE patterns of Carboniferous metagranites also indicate relatively garnet-free mantle source (Martin, 1993; Wilson, 1989).

The trace element contents of the metagranite samples fall within volcanic arc environment in the Nb versus Y and Rb versus Y + Nb diagrams of Pearce et al. (1984) and Pearce (1996). In evaluated Rb vs. Y + Nb binary diagram (Förster et al., 1997) upper part of the VAG field corresponds to continental arc setting (Fig. 8a–b). The Th/Yb and Ta/Yb ratios of the metagranites fall into high Th/Yb field near active continental arc environment on the binary diagram indicating the influence of Th enriched subduction fluids or crustal interaction and contamination (cf. Wilson, 1989, the geochemical plots from Pearce, 1983) (Fig. 9).

5. Geochronology and trace element chemistry of zircons

Six samples from the metagranites (samples 2073 and 2243 from the granoblastic metagranites, and 2089, 2093 and 2240 from the porphyritic metagranites) and one metaconglomerate sample from the Lower Triassic basal quartz metaconglomerate (sample 2275) were dated by U-Pb zircon geochronology using LA-ICP-MS (Analytical details for zircon separation and LA-ICP-MS measurements are given in

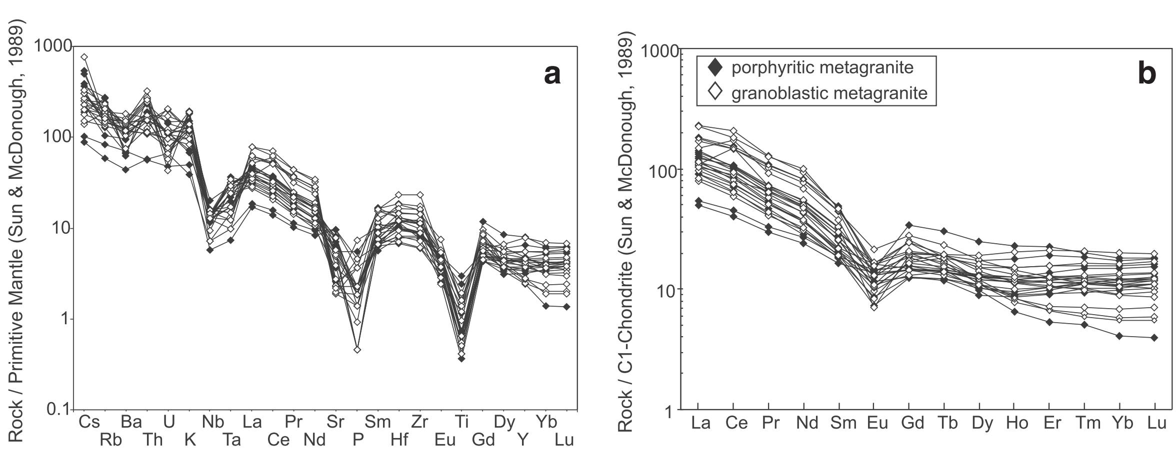

Fig. 7. a) Primitive mantle-normalized trace element spidergrams and b) chondrite-normalized rare earth element diagrams of the metagranites. The normalization values of primitive mantle and chondrite are after Sun and McDonough (1989).

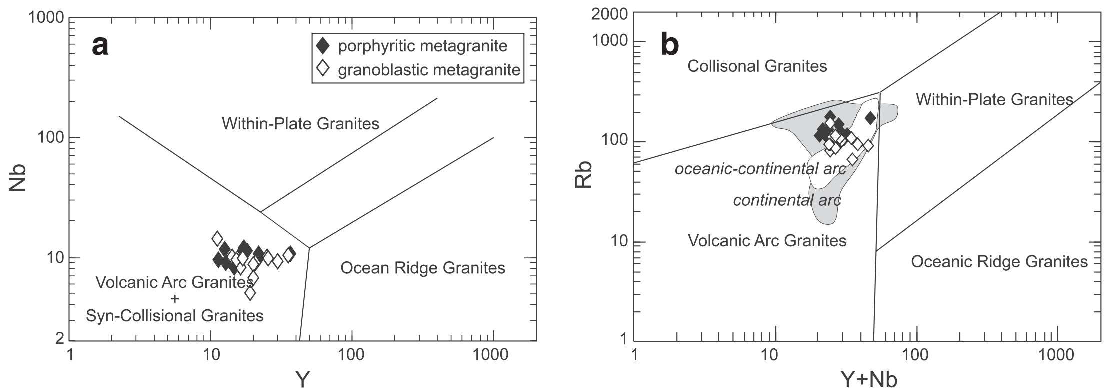

Fig. 8. a–b) Tectonic discrimination trace element diagrams of Pearce (1996) showing Nb vs. Y and Rb vs. Y + Nb (concentrations in μg/g).

Supplementary material 1). Zircon morphologies and age interpretations are given in Fig. 10 and in the Tables 2 and 3 (Supplementary material 3 and 4), respectively. Only ages between 95% and 105% concordance are used for calculation and interpretation.

5.1. Granoblastic metagranites

Dated samples are medium-grained rocks and consist of quartz, plagioclase, orthoclase, muscovite, chlorite and epidote with accessory zircon and apatite. They show mylonitic foliation defined by preferentially alignment of metamorphic white mica, chlorite and quartz.

5.1.1. Sample 2073 (coordinates: 35 S 0636581-434778)

Ten points from ten zircon grains were analyzed (Table 2). The main zircon population plots on the concordia curve between 310 and 330 Ma. One analysis, which yields discordant age (grain 8; <95% concordant) was not used for age calculation. Nine analyses yield a concordia age of 321.9 ± 2.6 Ma (MSWD = 0.59), which is very similar to the $^{206}Pb/^{238}U$ weighted average age of 321.1 ± 5.3 Ma (1σ, MSWD = 0.74; 95% confidence; Fig. 11a). The concordia age of 321.9 ± 2.6 Ma can be taken as the initial crystallization age of the granoblastic metagranite.

5.1.2. Sample 2243 (coordinates: 35 S 0634627-4351463)

Twenty-one points from 21 zircon grains were analyzed (Table 2). The main zircon population clusters along the concordia curve between 300 and 340 Ma. Two analyses of the sample yielding discordant ages (grains 7 and 18; <95% concordant) were omitted from age calculation. Seventeen analyses yield identical concordia and $^{206}Pb/^{238}U$ weighted mean ages of 320.5 ± 2.5 Ma (MSWD = 0.9) and 320.7 ± 6.3 Ma (1σ, MSWD = 1.4; 95% confidence), respectively (Fig. 11b). Four analyses from core domains gave older ages ranging from 586 Ma to 608 Ma. The concordia age of 320.5 ± 2.5 Ma is interpreted as crystallization age of the protolith of granoblastic metagranite, which is within error limits the same as the age from the sample 2073.

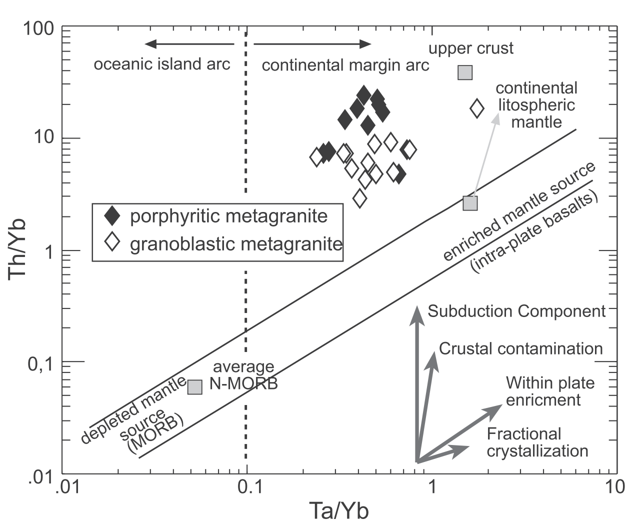

Fig. 9. Th/Yb vs. Ta/Yb rations of the metagranites plotted in the active margin continental arc field (Pearce, 1983).

5.2. Porphyritic metagranites

The porphyritic metagranite samples are composed of quartz, plagioclase, orthoclase, muscovite, chlorite and epidote with accessory zircon and apatite. They are coarse-grained rocks with blastomylonitic texture.

5.2.1. Sample 2089 (coordinates: 35 S 0635021-4350518)

A total of 21 analyses were performed on magmatic domains of zircon grains (Table 2). Three analyses of the sample yield discordant ages, reflecting probably variable Pb loss, (grains 2–4; <95% concordant) and they were not used for age calculation. Other zircons have consistent $^{206}Pb/^{238}U$ ages ranging from 309 Ma to 349 Ma. The remaining 18 analyses yield a concordia age of 325.8 ± 2.3 Ma (MSWD = 0.9), which can be interpreted as the crystallization age of the protolith of porphyritic metagranite (Fig. 11c). Additionally, they yield a $^{206}Pb/^{238}U$ weighted mean age of 326.2 ± 5.8 Ma (1σ, MSWD = 1.2, n = 18).

5.2.2. Sample 2093 (coordinates: 35 S 0635426-4351875)

To determine the emplacement ages of the original granite, forty-two zircons showing oscillatory zoning were analyzed (Table 2). The main zircon population clusters along the concordia curve between 320 and 340 Ma. Thirty-four analyses yield a $^{206}Pb/^{238}U$ weighted mean age of 331.3 ± 1.7 Ma (1σ, MSWD = 1.4; 95% confidence; Fig.11d). This age is interpreted to reflect the age of crystallization for the protolith of porphyritic metagranite. Inherited ages obtained from the cores of the zircons range from 1863 Ma to 431 Ma.

5.2.3. Sample 2240 (coordinates: 35 S 0632975-4347840)

A total of seventeen analyses were conducted on magmatic domains of zircon grains (Table 2). All of the zircons have consistent $^{206}Pb/^{238}U$ ages ranging from 300 Ma to 329 Ma. They yield a concordia age of 314.9 ± 2.4 Ma (MSWD = 1.3) and a $^{206}Pb/^{238}U$ weighted mean age of 314.3 ± 4.8 Ma (1σ, MSWD = 0.6; 95% confidence; Fig. 11e). The concordia age of 314.9 ± 2.4 Ma is interpreted as crystallization age of the protolith of porphyritic metagranite.

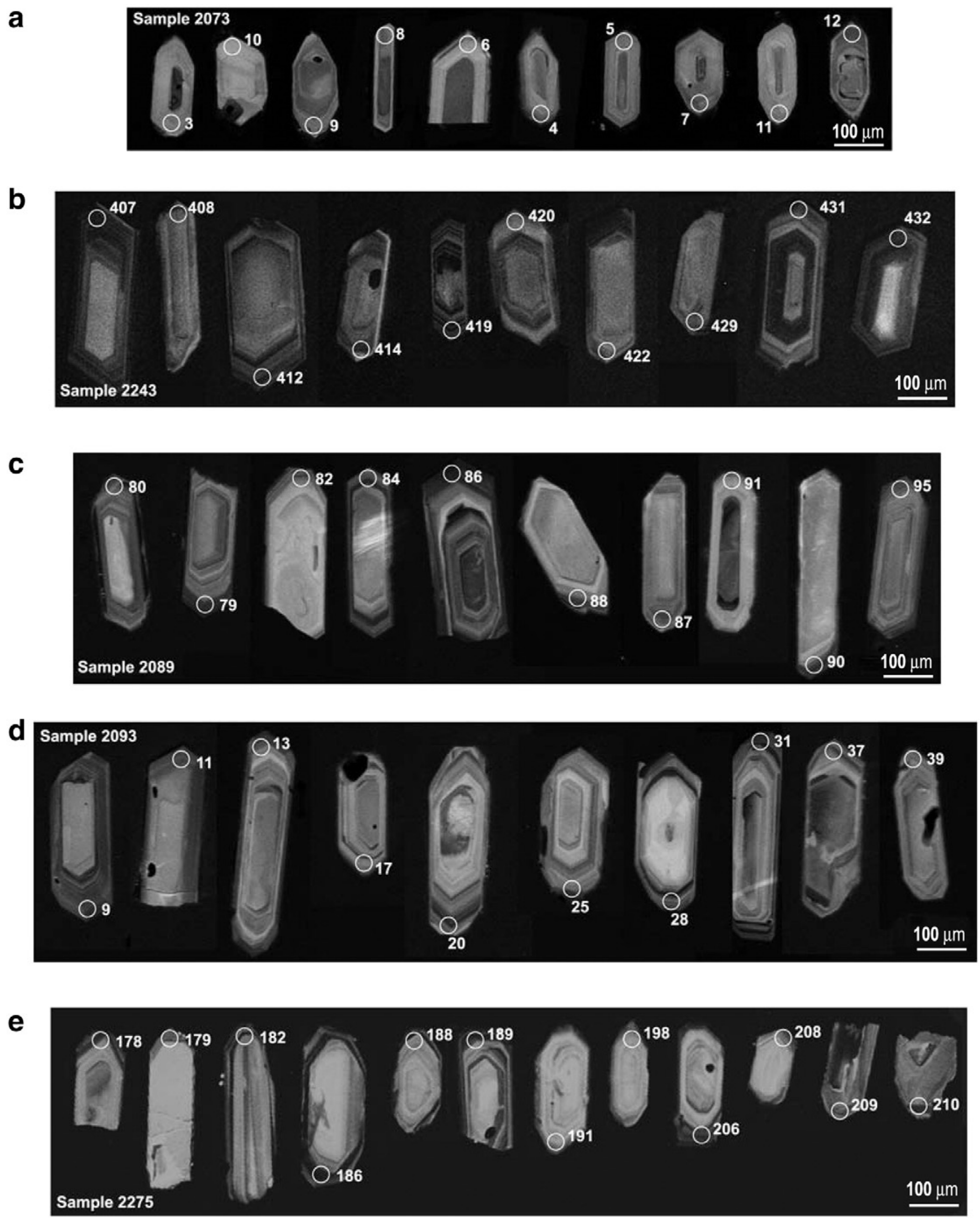

Fig. 10. Representative cathodoluminesence images of zircon grains from dated samples showing typical zoning of igneous crystallization. The locations and numbers of LA ICP-MS spot analyses are marked on zircons. a–b) Granoblastic metagranites; 2073–2243, c–d) porphyritic metagranites; 2089–2093 and e) quartz metaconglomerate; 2275.

5.3. Quartz metaconglomerate

This sample was taken from quartz-rich sandy parts of the quartz metaconglomerate lying on the Carboniferous granites. It consists of quartz, plagioclase and white mica with accessory zircon, apatite and opaque minerals.

5.3.1. Sample 2275 (coordinates: 35 S 0633194-4349670)

Twenty-seven analyses were performed on 24 detrital zircon grains. The ages range between Neoproterozoic and Late Permian (20 grains, 74%; Table 3), and show three age groups at *c.* 319, 478 and 818 Ma in the relative probability diagram (Fig. 12a–b). The pronounced symmetric peak at 319 Ma is well consistent with the crystallization ages of the Carboniferous granites in the underlying basement. Two individual Devonian (363 and 369 Ma) and two Early Ordovician (471 and 478 Ma) and two Late Cambrian ages (493 and 507 Ma) form the second group. Additionally, two oldest grains yielded Neoproterozoic ages (812 and 816 Ma).

The trace element compositions of zircons from representative samples of 2073 and 2093 of granoblastic metagranite and porphyritic metagranite, respectively, were measured (Table 4). The Th/U ratios range between 0.1 and 1, and the REE patterns show overlap with igneous zircons (Rubatto, 2002; Hoskin and Schaltegger, 2003; Kirkland et al., 2015). Total REE abundances of the zircons are high and vary from 327 µg/g to 3742 µg/g (Fig. 13a-b), which are typical for crustal igneous rocks (Hoskin and Schaltegger, 2003). The C1-chondrite normalized REE patterns of zircon trace elements show regular steeply-rising

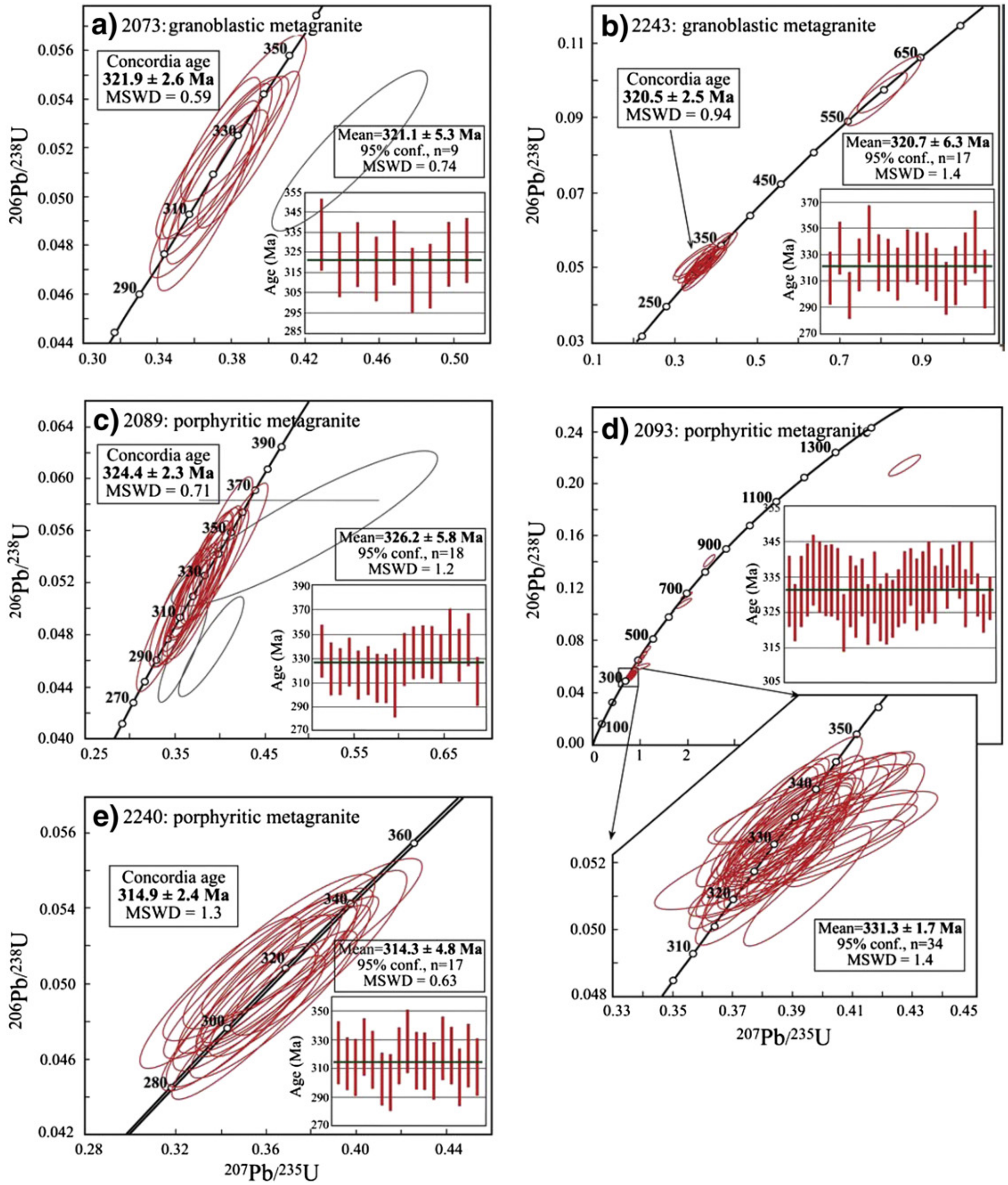

Fig. 11. a–e) U-Pb concordia diagrams and weighted average ages of zircons from granoblastic metagranites and porphyritic metagranites.

slope from the LREE to the HREE with negative-Eu anomaly and positive Ce-anomaly, which are consistent with zircons crystallized in igneous conditions (Hoskin and Schaltegger, 2003). Negative Eu anomalies indicate coeval feldspar crystallization.

6. Discussion

Here we describe metagranites with Early to mid-Carboniferous (331–315 Ma) crystallization ages from the Afyon zone on the northern margin of the Anatolide-Tauride Block. They indicate a continental arc setting and underwent metamorphism and deformation at the Cretaceous-Tertiary boundary. These Carboniferous granites from the Anatolide-Tauride Block raise several questions, which are discussed below.

6.1. The problems of genetic classification of metagranites from the Afyon zone

Generally, granitic rocks can be assigned to two dominant genetic groups, I- and S-type (Chappell and White, 1974), with different chemical and mineralogical composition being dominantly derived from igneous and metasedimentary source rocks, respectively (Chappell, 1984). When we use this traditional approach for the genetic classification of the metagranites from the Afyon zone, we arrive to somehow contradictory conclusions: at the first glance, the metagranites show peraluminous character (Fig. 6b), resembling S-type granites of Chappell and White (1974), and suggesting dominantly intracrustal derivation, typical for a collisional environment. However, there are other lines of evidence which argue against an S-type affinity. The most important one is the considerable consistency of the zircon age

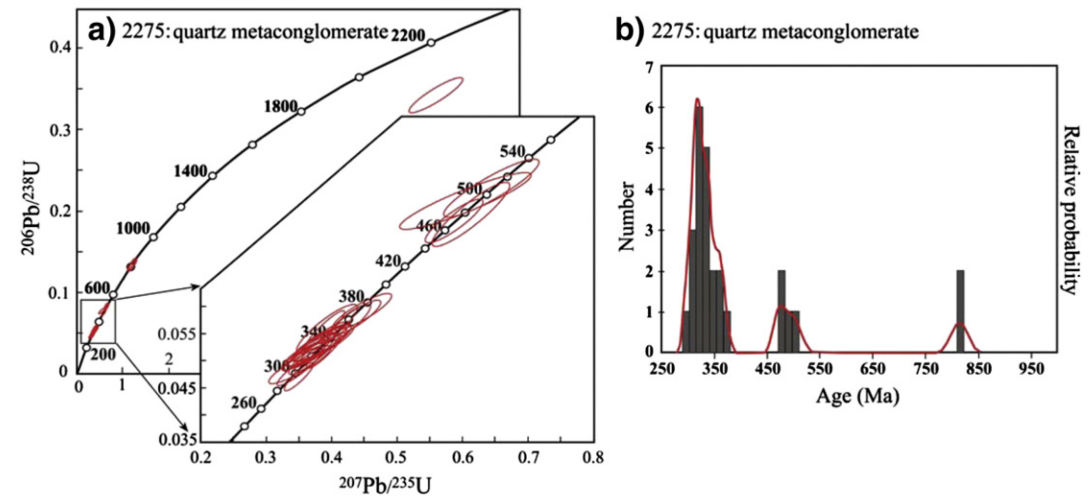

Fig. 12. a) Concordia diagram and b) probability density distribution plot for the set of U-Pb zircon data from quartz metaconglomerate (sample number 2275).

data, with negligible amount of inherited grains derived from the basement rocks. This is peculiar, because for an S-type origin of the metagranites from the Afyon zone, several distinctive zircon populations reflecting age distribution inherited from their metasedimentary protolith would be expected. One possibility is that primary polygenetic zircon populations derived from a metasedimentary source could have been isotopically reset at high temperature during the subsequent melting event. However, Ti-in-zircon temperature estimations suggest relatively low zircon crystallization temperatures ranging between 650–750 °C (Fig. 14a) (Supplementary material 5), whereas temperatures >900 °C are needed for resetting of zircons (Lee et al., 1997).

Alternatively, the high silica contents exceeding 70% for all granitic samples may result after considerable fractionation. Extremely low CaO contents as well as a decrease of alumina index in the most evolved samples, together with Eu anomaly in zircon, suggest that the major fractionating phase was plagioclase (Fig. 14b). Moreover, the Zr variations also demonstrate fractionation control, and broadly plot along the expected fractionation curve (Fig. 14c). The least silica rich samples show the highest Zr and highest Dy/Yb ratios, which may be interpreted as a consequence of the presence of the garnet in the source (Fig. 14d). The experiments on the basaltic starting material at the pressures >10 kbar demonstrate that the restites will universally be rich in garnet, and this corresponds to the melting of the mafic lower crust of garnet-amphibolitic compositions at the base of the crust (e.g. Qian & Hermann, 2013 and references therein), which is typical for magma generation and evolution in continental arc settings.

In summary, the Early-Middle Carboniferous granitic rocks has been formed either by high-degree differentiation of mafic calc-alkaline melts, or (more likely) by partial melting of metaluminous amphibolitic sources influenced by subduction related processes within the lower crust.

6.2. Comparison of the Carboniferous tectono-thermal events on southern margin of Laurasia and on the northern margin of Gondwana

Lower to mid-Carboniferous granites of the Afyon zone occur in the Anatolide-Tauride block (Figs. 1 and 2), which was separated from northern margin of Gondwana by the opening of the southern branch of Neotethys in Early Triassic and accreted to the southern margin of Laurasia along the İzmir-Ankara suture by the Tertiary collision (Şengör et al., 1980; Şengör and Yılmaz, 1981). However, in contrast to this widely accepted view, in some paleogeographic reconstructions for Late Palaeozoic, Anatolides, as well as the Afyon zone, is placed on the active northern margin of the Paleotethys along the southern margin of Laurasia in the same position with the Pelagonian zone in Greece and Sakarya zone of Pontides (Stampfli et al., 2013 and references therein). The Sakarya zone north of the İzmir-Ankara suture (Fig. 15a–b), which is assumed to have been separated from northern margin of the Gondwana in Early Paleozoic (Ustaömer et al., 2012b; Stampfli et al., 2013; Okay and Nikishin, 2015) or Early Triassic (Göncüoğlu, 2011) is characterized by Upper Jurassic to Cretaceous sedimentary and volcanic rocks covering unconformably a tectonically

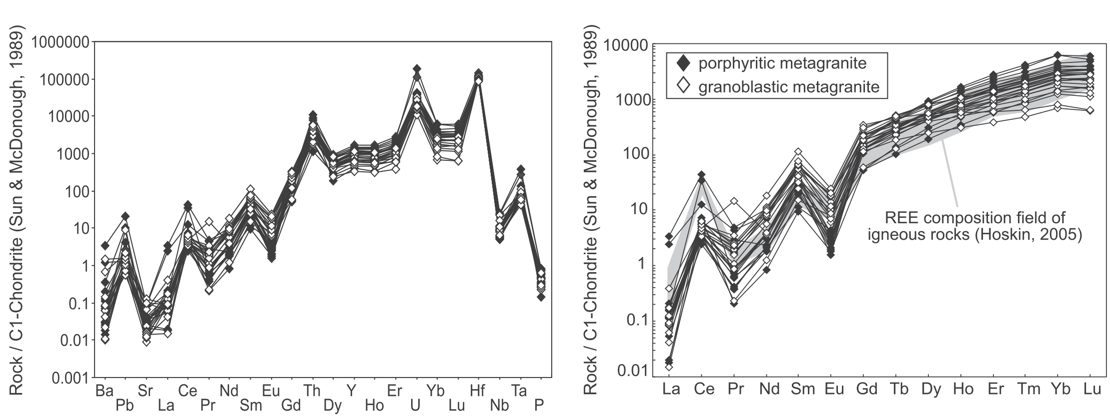

Fig. 13. C1 chondrite-normalized (Sun and McDonough, 1989) trace element (A) and REE (B) patterns for representative zircons of porphyritic and granoblastic metagranites.

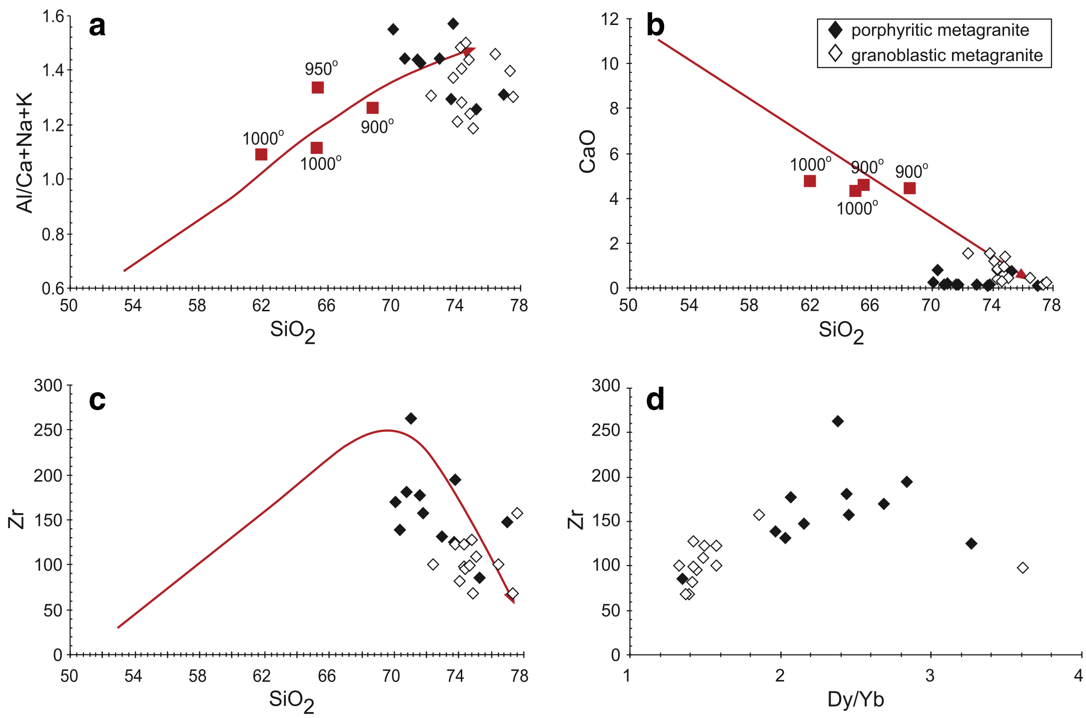

Fig. 14. a–d) Plots of Aluminium Saturation Index, Ca and Zr versus SiO2, and Zr versus Dy/Yb for Afyon zone metagranites. Arrows define the fractionation paths recognized in typical I-type granites from Lachlan Fold belt, Australia (Chappell et al., 2012), generated by substantial partial melting of more mafic source rocks and subsequent fractional crystallization. Red stars represent experimental melts of basaltic starting material at 12 kbar (Zhang et al., 2013), and the numbers define the melting temperatures (oxides are given in wt.%, element concentrations in μg/g).

juxtaposed heterogeneous basement with complex tectono-thermal history related to Variscan (Carboniferous), Cimmeride (Triassic eclogites and blueschists; Okay et al., 2002; Okay and Göncüoğlu, 2004), and Alpine (Jurassic magmatism, Şen, 2007; Okay and Nikishin, 2015 and associated LP/HT metamorphism, Okay et al., 2014a, b) orogenies. Carboniferous LP/HT metamorphic rocks of the Sakarya zone (*c.* 310–330 Ma; Topuz et al., 2004, 2007; Ustaömer et al., 2012b) and associated Lower to mid-Carboniferous granitoids (*c.* 320–330 Ma; Topuz et al., 2010; Ustaömer et al., 2012a, b) have been well documented and are interpreted as the effects of the Variscan orogeny in the Pontides (Ustaömer et al., 2012a, b; Okay and Nikishin, 2015 and references therein). However, the tectonic setting of this Carboniferous tectono-thermal event is still controversial. In one interpretation involving southward subduction of the Paleotethys beneath the Gondwana, Variscan arc magmatism and associated metamorphism took place along the northern margin of Gondwana (Şengör and Yılmaz, 1981; Yılmaz et al., 1997; Xypolias et al., 2006; Göncüoğlu et al., 2007; Göncüoğlu, 2011). But, the absence of a Paleotethyan suture to the north of Sakarya zone (Okay, 2000; Topuz et al., 2013) is inconsistent with this model. In a different model, the Variscan event in the Pontides is attributed to the northward subduction of the Paleotethys and development of an Andean-type active margin along the southern margin of Laurasia (Robertson and Dixon, 1984; Robertson et al., 1996; Vavassis et al., 2000; Ustaömer et al., 2012b; Stampfli and Borel, 2002; Stampfli et al., 2001). More recently, a new tectonic model involving the southward subduction of the Rheic Ocean under a ribbon-shaped continental block including Rhodope, Sakarya Zone and Caucasus, development of a continental arc and Late Carboniferous collision with the southern margin of Laurasia has been suggested for the Variscan evolution of the Pontides (Okay et al., 2006; Okay and Nikishin, 2015). Similarly, pre-Alpine metamorphic basement of Pelagonian zone and Cycladic complex contain mid-Carboniferous to Lower Permian granite intrusions (*c.* 315–275 Ma; Engel and Reischmann, 1998; Reischmann, 1998; Reischmann et al., 2001; Anders et al., 2007; Schenker et al., 2014) and associated medium to high-grade metamorphic rocks (Okrusch and Bröcker, 1990; Vavassis et al., 2000; Most, 2003; Mposkos et al., 2001; Mposkos and Krohe, 2004). This tectonothermal event is assigned to Variscan orogeny in the Balkans (De Bono, 1998; Vavassis et al., 2000; Most, 2003; von Raumer and Stampfli, 2008; Stampfli et al., 2013; Schenker et al., 2014). This Late Carboniferous event extents to central European Variscides in the west (magmatic activity: *c.* 400–250 Ma; Bonin et al., 1993; Finger et al., 1997; Kroner and Romer, 2013 and metamorphism: *c.* 400–340 Ma; Stosch and Lugmair, 1990; Kröner et al., 2000; Rötzler and Romer, 2001; Roger and Matte, 2005; Moita et al., 2005; Ballèvre et al., 2009; Berger et al., 2010; Godard, 2009; Bröcker et al., 2009; Kroner and Romer, 2013) and the Caucasus in the east (metamorphism: *c.* 330 Ma and magmatism: *c.* 330–270 Ma, Mayringer et al., 2011; Rolland et al., 2011) (Fig. 15a–b).

The Anatolide-Tauride Block, however, is made up of a Late Proterozoic Pan-African basement and unconformably overlying Cambrian to Tertiary series (Özgül, 1976; Candan et al., 2011). The Palaeozoic stratigraphy of the Anatolide – Tauride Block shows great similarities to that of Arabian Plate (Özgül, 1984; Göncüoğlu and Kozlu, 2000; Ghienne et al., 2010 and references therein). In the Anatolides, the Lower Triassic sequence starts with coarse-grained continental clastic sediments interfingering laterally with volcanics (Akal et al., 2012; Candan et al., 2005; Konak et al., 1987) and passes upwards to shallow marine shales. Upper Triassic to Late Cretaceous sequence is characterized by a continuous platform-type thick carbonate deposition (Özgül, 1984) and is free of Jurassic magmatism. Except for Late Proterozoic basements evolved during the Pan-African events (Candan et al., 2016; Koralay et al., 2012), there is no evidence for pre-Cretaceous deformation and metamorphism in Anatolides (Okay et al., 2006; Sherlock et al., 1999; Pourteau et al., 2013; Bozkurt and Satır, 2000). In Simav area, where the stratigraphy is similar to that of the Anatolide-Tauride block, there are no differences in the metamorphic grade between basement and the cover series. Structural and textural evidence indicate a single-stage Alpine deformation and metamorphism for the region. Thus, the Late Palaeozoic – Early Tertiary stratigraphy and tectono-thermal evolution of the Afyon zone are strikingly different from that of the Sakarya

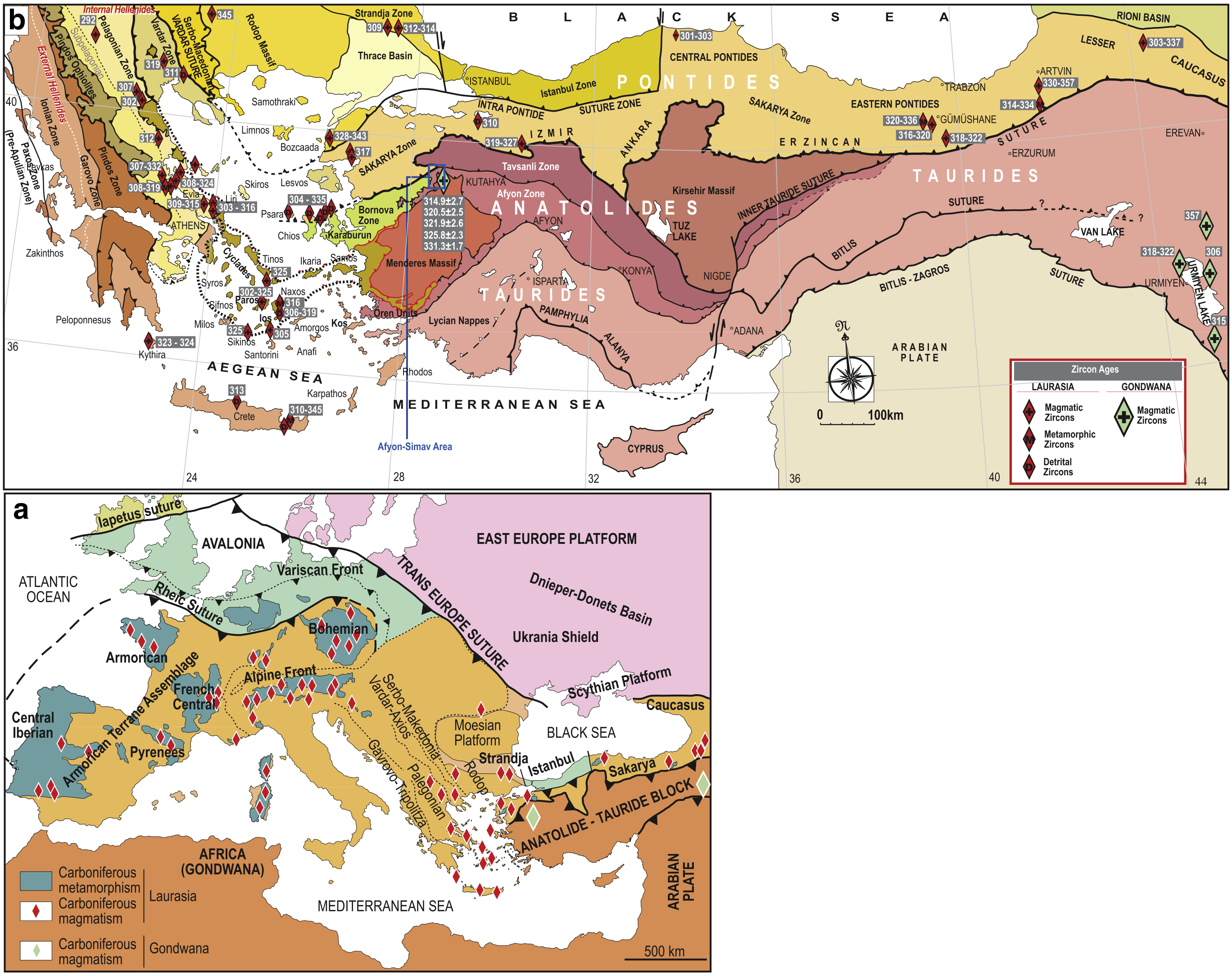

Fig. 15. a) General distribution of Carboniferous to Permian magmatic and metamorphic rocks in Laurasia and Gondwana. Carboniferous granites of the Afyon zone occur on the northern margin of Gondwana (modified from Okay and Tüysüz, 1999; Keay and Lister, 2002; Himmerkus et al., 2009; Jolivet et al., 2010; Jolivet and Brun, 2010; Philippon et al., 2012; Chatzaras et al., 2013; Papanikolaou, 2013; Pourteau et al., 2013; Kydonakis et al., 2014; Schenker et al., 2014; Çetinkaplan et al., 2016). Granite localities in Iran are from Bea et al. (2011); Alirezaei and Hassanzadeh (2012); Saccani et al. (2013); Moghadam et al. (2015). b) Igneous, metamorphic and detrital Carboniferous to Permian zircon ages on Greece, Turkey and Iran.

and Pelagonian zones. Although the Carboniferous magmatic activity in the Afyon zone suggests a temporal relation to the Variscan orogeny identified along the southern margin of Laurasia, the geological evidence indicates the northern Gondwanan affinity of the Afyon zone and precludes a causal relation with Variscan orogeny of these granites.

6.3. Late Palaeozoic subduction history of Paleotethys

Palaeotethys is considered as an ocean, which was opened on the northern margin of Gondwana in Early Devonian (von Raumer and Stampfli, 2008; Stampfli et al., 2013). However, there are considerable debates regarding the Late Palaeozoic tectonic setting of Gondwana-related southern margin and subduction polarity of this ocean (Robertson and Ustaömer, 2009a, b and references therein). Three tectonic models have been suggested for the closure history of the Paleotethys; *i*) northward subduction under Laurasia, with a location of Paleotethys to the south (Robertson and Dixon, 1984; Robertson et al., 1996; Ustaömer and Robertson, 1993; Zanchi et al., 2003; Okay et al., 2006; von Raumer et al., 2013; Stampfli and Borel, 2002; Stampfli et al., 2013; Eren et al., 2004), *ii*) southward subduction under Gondwana, with Paleotethys to the north (Şengör, 1979; Şengör et al., 1980; Şengör and Yılmaz, 1981; Göncüoğlu et al., 2003, 2007; Romano et al., 2006; Xypolias et al., 2006; Zulauf et al., 2007; Akal et al., 2011a, b, 2012) and *iii*) double subduction both southward and northward that Paleotethys is placed between Gondwana and Laurasia (Robertson and Ustaömer, 2009b, 2011). As discussed above, in the Sakarya zone of the Pontides there are episodic magmatic - metamorphic events ascribed to the Variscan, Cimmeride and Alpine orogenies along the active southern margin of Laurasia (Stampfli et al., 2013; Topuz et al., 2013; Okay and Nikishin, 2015 and references therein). Apart from the Carboniferous arc-type granites described in the Afyon zone, mélange-type Carboniferous units on Chios Island, Karaburun and Konya on the northern margin of the Anatolide-Tauride Block (Zanchi et al., 2003; Meinhold and Frei, 2008; Robertson and Ustaömer, 2009a, b; Göncüoğlu et al., 2007; Robertson and Pickett, 2000), which have formed by subduction-accretion processes (Robertson and Ustaömer, 2009a, b) are of significance regarding the subduction polarity of the Paleotethys. Detrital zircons from Chios mélange include Carboniferous ages of 360–320 Ma (Meinhold et al., 2008), which have been used to place Chios on the southern margin of Laurasia. However, the ages of the Lower to mid-Carboniferous granites in Simav area overlap with the zircon ages from Chios, and indicate an alternative source area with northern Gondwanan affinity for Chios mélange. Furthermore, Chios, Karaburun and Konya mélanges are all stratigraphically overlain by similar Mesozoic sequences. On the Chios Island, Carboniferous mélange is unconformably overlain by Lower Triassic to Jurassic clastic sediments and platform-type carbonates (Robertson and Pickett, 2000; Zanchi et al., 2003). Similarly, in Karaburun, the mélange is overlain unconformably by an intact Lower Triassic to Cretaceous carbonate-dominated succession showing marked similarities with the Anatolide-Tauride platform (Kozur, 1997; Robertson and Pickett, 2000; Stampfli et al., 2003; Çakmakoğlu and Bilgin, 2006). In Konya area the Carboniferous mélange is unconformably overlain by Upper Permian platform carbonates with a fauna of Gondwanan affinity (Altıner et al., 2000; Özcan et al., 1988; Göncüoğlu et al., 2007), which are unconformably succeeded by a Lower Triassic to Cretaceous coherent sequence (Özcan et al., 1988; Akal et al., 2011b). Therefore, stratigraphic evidence from the Mesozoic cover series of mélanges combined with the arc-type Carboniferous plutons suggest southward subduction of the Paleotethys under Gondwana during the Carboniferous.

Overall, a northward subduction under Laurasia from Carboniferous to the Late Mesozoic as defined by the presence of Carboniferous LP-HT metamorphism - plutonism and Triassic, Jurassic and Cretaceous subduction-accretion complexes has been documented in the Sakarya zone of the Pontides (Stampfli et al., 2013; Topuz et al., 2013; Okay and Nikishin, 2015). Additionally, the presence of Carboniferous subduction-accretion complexes and arc-type granites on the northern margin of the Anatolide-Tauride Block also suggest southward subduction under Gondwana. Therefore, during the Carboniferous the Paleotethys was subducting both north under Laurasia and south under Gondwana. The southward subduction might have been responsible for the initiation of rifting leading to the separation of the Anatolide-Tauride Block from the main trunk of Gondwana (Fig. 16a–c).

6.4. Tectonic scenario

Similar to the closure models suggested for the Rheic (Stampfli et al., 2013; von Raumer and Stampfli, 2008) and the Neotethys (Hässig et al., 2015) oceans, the geological evidence favors dual subduction both under Laurasia and Gondwana for the Paleotethys during Late Palaeozoic (Fig. 16a). Considering the age of the matrix of the mélanges (Early-mid Carboniferous) and the intrusion age of the subduction-related granites (Early-mid-Carboniferous), the southward subduction under Gondwana was, however, short-lived. In the Late Permian a shallow marine carbonate platform with a basal quartzite horizon representing establishment of a passive continental margin setting was deposited on the Carboniferous mélanges, and during the Mesozoic

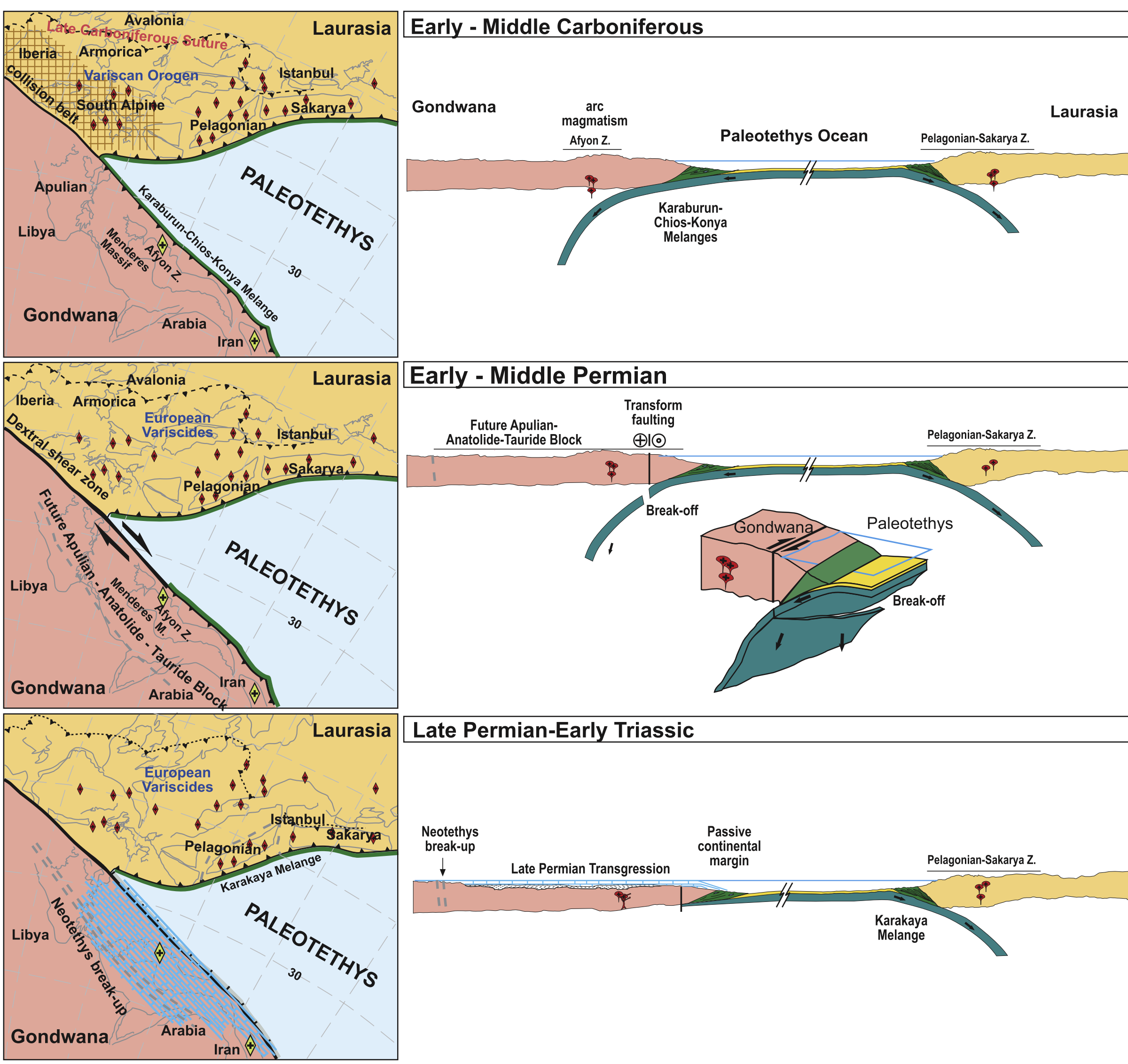

Fig. 16. a–c) Tectonic model for Late Palaeozoic tectonic evolution of Paleotethys discussed in the paper. Paleogeographic maps are based on the Early Carboniferous tectonic reconstructions after Vavassis et al. (2000), Stampfli and Kozur (2006), Robertson and Ustaömer (2009a, b); Torsvik and Cocks (2013).

there is no evidence for subduction-related magmatism or metamorphism on the northern margin of Gondwana in the Anatolian transect. Thus, the southward subduction under Gondwana can be constrained between Early Carboniferous and Late Permian.

Geological evidence indicating the existence of an accreted continental block by the collision along the northeastern margin of Gondwana during the Late Palaeozoic is unknown. Thus, the mechanism accounting for the transition from subduction to passive continental margin setting for southern margin of Paleotethys remains speculative. Similar to the tectonic model suggested for termination of subduction-related Cadomian orogeny without following a continental collision (Linnemann et al., 2007), a tectonic scenario involving an oblique subduction, a gradual transition to a transform plate margin setting and slab break-off, similar to present-day geodynamics of North American plate system (McCrory et al., 2009) can be envisaged for the southern margin of the Paleotethys (Fig.16b). However, considering the available geological data, a mechanism involving change from transform to passive plate margin setting remains an open question.

Another possibility involving the Late Palaeozoic global plate organization in the context of Variscan Orogeny and final assembly of Pangea can be considered. In general, the closure of the Rheic Ocean is accepted to have started diachronously with the Early Carboniferous collision of Gondwana-derived ribbon terranes with Laurasia in Europe and continued into Permian with the collision of Laurasia along the West African margin of Gondwana to form Pangea (Hatcher, 2002; von Raumer and Stampfli, 2008; Nance et al., 2010; Stampfli et al., 2013; Kroner and Romer, 2013). The termination of the southward subduction of the Paleotethys and establishment of a passive continental margin setting suggested by this study coincides well with the final collision between Gondwana and Laurasia Furthermore, it is suggested that after the termination of the Variscan orogeny during the plate reorganization (i.e. transformation from Pangea B to Pangea A; Muttoni et al., 2003, 2009) at *c.* 300–250 Ma, the Gondwana plate decoupled from European Variscides along the Intra-Pangea dextral shear zone, which constituted a transform plate boundary in response to the relative motion between Gondwana and Laurasia (Fig. 16a; Veevers, 2004; Robertson, 2006; Kroner and Romer, 2013). Although no structural evidence has been documented on the eastward extension of this transform plate boundary along the northern margin of Gondwana, most probably because of the strong Alpine deformation, the change of tectonic setting from subduction to transform plate boundary can be ascribed to this global plate boundary reorganization (Fig. 6b). Eastward migration of this transform plate boundary may have been accompanied by slab break-off of the subducted oceanic plate (Fig. 16b) and, subsequently, sinking of the slab as a consequence of the densification/eclogitization of the oceanic lithosphere and pull forces (Duesterhoeft et al., 2014). This process continued until the Late Permian and, finally, should have switched to a passive continental margin prior to Late Permian regional transgression on the northern margin of Gondwana (Fig. 16c). The gradual transition from transform plate boundary to passive margin setting, most probably, can be assigned to the termination of the convergence regime between Laurasia and Gondwana along the Variscan orogenic belt during the final assembly of Pangea (Early Permian-Early Triassic; Muttoni et al., 2003; Stampfli and Borel, 2002). The original tectonic zonation, Carboniferous mélange and arc magmatism, indicating southward subduction of the Paleotethys beneath the Gondwana, however, should have been disrupted by the Late Cretaceous-Eocene collision between Anatolide-Tauride block and Pontides in response to the closure of the northern branch of Neotethys (Okay et al., 2001).

7. Conclusions

Pre-Triassic basement of the Afyon zone, probably Infra-Cambrian in age, is intruded by granite bodies, which were converted to mylonitic metagranites during the low-grade Alpine metamorphism. Geochemical characteristics of these granites, which are dated at 331 Ma to 315 Ma (Early to Middle Carboniferous), indicate a continental arc setting developed along the active northern margin of Gondwana. Furthermore, the widespread Carboniferous magmatism and associated metamorphism in Pelagonian and Sakarya zones, which are ascribed to northward subduction of the Paleotethys beneath southern margin of Laurasia allows us to suggest a dual subduction both southward and northward for Paleotethys. This short-lived southward subduction history of the Paleotethys along the northern margin of Gondwana can be constrained between Early Carboniferous and Late Permian. In the Late Permian, the active northern margin of Gondwana should have switched to a passive continental margin setting by a transform plate boundary stage, which can be assigned to the termination of the convergence regime between Gondwana and Laurasia during the late stage of Pangea formation.

Supplementary data to this article can be found online at http://dx.doi.org/10.1016/j.tecto.2016.06.030.

Acknowledgments

This work was financially supported by research grants from the Scientific and Technological Research Council of Turkey (TÜBITAK; project no: 109Y144). The support of the granting agency is warmly acknowledged.

References

Akal, C., Candan, O., Koralay, O.E., Okay, A.I., Oberhänsli, R., Chen, F., 2011a. Geochronology, geochemistry and geology of the Devonian granites in Afyon Zone, north of Simav. TÜBİTAK Project 109Y144 (in Turkish with English abstract, 247 pp).
Akal, C., Koralay, O.E., Candan, O., Oberhänsli, R., Chen, F., 2011b. Geodynamic significance of the Early Triassic Karaburun granitoid (Western Turkey) for the opening history of Neo-Tethys. Turk. J. Earth Sci. 20, 255–271.
Akal, C., Candan, O., Koralay, O.E., Oberhänsli, R., Chen, F., Prelevic, D., 2012. Early Triassic potassic volcanism in the Afyon Zone of the anatolides/Turkey: implications for the rifting of the Neo-Tethys. Int. J. Earth Sci. 101, 177–194.
Alirezaei, S., Hassanzadeh, J., 2012. Geochemistry and zircon geochronology of the Permian A-type Hasanrobat granite, Sanandaj–Sirjan belt: a new record of the Gondwana break-up in Iran. Lithos 151, 122–134.
Altıner, D., Özcan-Altıner, S., Koçyiğit, A., 2000. Late Permian foraminiferal biofacies belts in Turkey: paleogeographic and tectonic implications. In: Bozkurt, E., Winchester, J.A., Piper, J.A.D. (Eds.), Tectonics and Magmatism in Turkey and the Surrounding Area. Geological Society, London, Special Publications 173, pp. 83–96.
Anders, B., Reischmann, T., Kostopoulos, D., Lehnert, O., Matukov, D., Sergeev, S., 2007. Zircon geochronology of basement rocks from the Pelagonian Zone, Greece: constraints on the pre-Alpine evolution of the westernmost Internal Hellenides. Int. J. Earth Sci. 96, 639–661.
Bailey, J.C., 1981. Geochemical criteria for a refined tectonic discrimination of orogenic andesites. Chem. Geol. 32 (1–2), 139–154.
Ballèvre, M., Bosse, V., Ducassou, C., Pitra, P., 2009. Palaeozoic history of the Armorican Massif: models for the tectonic evolution of the suture zones. Tectonics 341, 174–201.
Bea, F., Mazhari, A., Montero, P., Amini, S., Ghalamghash, J., 2011. Zircon dating, Sr and Nd isotopes and element geochemistry of the Khalifan pluton, NW Iran: evidence for Variscan magmatism in a supposedly Cimmerian superterrane. J. Asian Earth Sci. 40, 172–179.
Berger, J., Féménias, O., Ohnenstetter, D., Bruguier, O., Plissart, G., Mercier, J.C.C., Demaiffe, D., 2010. New occurrence of UHP eclogites in Limousin (French Massif Central): age, tectonic setting and fluid–rock interactions. Lithos 118, 365–382.
Bonin, B., Brändlein, P., Bussy, F., Desmons, J., Eggenberger, U., Finger, F., Graf, K., Marr, C., Mercolli, I., Oberhänsli, R., Ploquin, A., Von Quadt, A., Von Raumer, J., Schaltegger, U., Steyerer, H.P., Visona, D., Vivier, G., 1993. Late Variscan magmatic evolution of the Alpine basement. The Pre-Mesozoic Geology in the Alps. Springer, pp. 169–199.
Bozkurt, E., Satır, M., 2000. The southern Menderes Massif (western Turkey): geochronology and exhumation history. Geol. J. 35, 285–296.
Bröcker, M., Klemd, R., Cosca, M., Brock, W., Larionov, A.N., Rodionov, N., 2009. The timing of eclogite facies metamorphism and migmatization in the Orlica–Œnienik complex, Bohemian Massif: constraints from a multimethod geochronological study. J. Metamorph. Geol. 27, 385–403.
Çakmakoğlu, A., Bilgin, Z.R., 2006. Pre-Neogene stratigraphy of the Karaburun Peninsula (W of İzmir Turkey). Bull. Mineral Res. Explor. 132, 33–62.
Candan, O., Dora, O.Ö., Oberhänsli, R., Oelsner, F., Dürr, S., 1997. Blueschist relics in the Mesozoic cover series of the Menderes Massif and correlations with Samos Island, Cyclades. Schweiz. Mineral. Petrogr. Mitt. 77, 95–97.
Candan, O., Çetinkaplan, M., Oberhänsli, R., Rimmele, G., Akal, C., 2005. Alpine high-pressure/low temperature metamorphism of Afyon Zone and implication for metamorphic evolution of western Anatolia, Turkey. Lithos 84, 102–124.
Candan, O., Koralay, O.E., Akal, C., Kaya, O., Oberhänsli, R., Dora, O.Ö., Konak, N., Chen, F., 2011. Supra-Pan-African unconformity between core and cover series of the Menderes Massif/Turkey and its geological implications. Precambrian Res. 184, 1–23.

Candan, O., Koralay, O.E., Topuz, G., Oberhansli, R., Fritz, H., Collins, A.S., Chen, F., 2016. Late Neoproterozoic gabbro emplacements followed by early Cambrian eclogite-facies metamorphism in the Menderes Massif (W. Turkey): Implications on the final assembly of Gondwana. Gondwana Res 34, 158–173.

Çetinkaplan, M., Pourteau, A., Candan, O., Koralay, O.E., Oberhänsli, R., Okay, A.I., Chen, F., Kozlu, H., Şengün, F., 2016. P-T-t evolution of eclogite/blueschist facies metamorphism in Alanya Massif: time and space relations with HP event in Bitlis Massif, Turkey. Int. J. Earth Sci. 105, 247–281.

Chappell, B.W., 1984. Source rocks of I- and S-type granites in the Lachlan Fold Belt, southeastern Australia. Philos. Trans. R. Soc. Lond. 310, 693–707.

Chappell, B.W., White, A.J.R., 1974. Two contrasting granite types. Pac. Geol. 8, 173–174.

Chappell, B.W., Bryant, C.J., Wyborn, D., 2012. Peraluminous I-type granites. Lithos 153, 142–153.

Chatzaras, V., Dörr, W., Finger, F., Xypolias, P., Zulauf, G., 2013. U–Pb single zircon ages and geochemistry of metagranitoid rocks in the Cycladic Blueschists (Evia Island): implications for the Triassic tectonic setting of Greece. Tectonophysics 595–596, 125–139.

Cox, K.G., Bell, R.J., Pankhurst, R.J., 1979. The Interpretation of Igneous Rocks. Allen and Unwin, London (450 pp).

De Bono, A., 1998. Pelagonian margins in central Evia Island (Greece). Stratigraphy and Geodynamic Evolution. Lausanne University (Unpublished PhD thesis). (114 pp).

Dora, O.Ö., Candan, O., Kaya, O., Koralay, O.E., Dürr, S., 2001. Revision of the so-called “leptite-gneisses” in the Menderes Massif: a supracrustal metasedimentary origin. Int. J. Earth Sci. 89 (4), 836–851.

Duesterhoeft, E., Quinteros, J., Oberhansli, R., Bousquet, R., de Capitani, C., 2014. Relative impact of mantle densitification and eclogitization of slabs on subduction dynamics: a numerical thermodynamic/thermokinematic investigation of metamorphic density evolution. Tectonophysics 637, 20–29.

Engel, M., Reischmann, T., 1998. Single zircon geochronology of orthogneisses from Paros, Greece. Bull. Geol. Soc. Greece 32 (3), 91–99.

Eren, Y., Kurt, H., Rosselet, F., Stampfli, G.M., 2004. Palaeozoic deformation and magmatism in the northern area of the Anatolide Block (Konya), witness of the Paleo-Tethys active margin. Eclogae Geol. Helv. 97, 293–306.

Finger, F., Roberts, M.P., Haunschmid, B., Schermaier, A., Steyrer, H.P., 1997. Variscan granitoids of central Europe: their typology, potential sources and tectonothermal relations. Mineral. Petrol. 61, 67–96.

Förster, H.J., Tischendorf, G., Trumbulla, R.B., 1997. An evaluation of the Rb vs. (Y + Nb) discrimination diagram to infer tectonic setting of silicic igneous rocks. Lithos 40, 261–293.

Ghienne, J.F., Monod, O., Kozlu, H., Dean, W.T., 2010. Cambrian–Ordovician depositional sequences in the Middle East: a perspective from Turkey. Earth-Sci. Rev. 3-4, 101–146.

Godard, G., 2009. Two orogenic cycles recorded in eclogite-facies gneiss from the southern Armorican Massif (France). Eur. J. Mineral. 21, 1173–1190.

Göncüoğlu, M.C., 2011. Geology of the Kütahya-Bolkardağ belt. Bull. Mineral Res. Explor. 142, 223–277.

Göncüoğlu, M.C., Kozlu, H., 2000. Early Paleozoic evolution of the NW Gondwanaland: data from southern Turkey and surrounding regions. Gondwana Res. 3, 315–324.

Göncüoğlu, M.C., Turhan, N., Tekin, K., 2003. Evidence for the Triassic rifting and opening of the Neotethyan İzmir-Ankara Ocean, northern edge of the Tauride-Anatolide Platform, Turkey. Bull. Geol. Soc. Ital. Spec. 2, 203–212.

Göncüoğlu, M.C., Çapkınoğlu, Ş., Gürsu, S., Noble, P., Turhan, N., Tekin, U.K., Okuyucu, C., Göncüoğlu, Y., 2007. The Mississippian in the central and eastern Taurides (Turkey): constraints on the tectonic setting of the Tauride–Anatolide Platform. Geol. Carpath. 58, 427–442.

Gürsu, S., Göncüoğlu, M.C., Turan, N., Kozlu, H., 2004. Characteristic features of Precambrian, Paleozoic and Lower Mesozoic successions of two different tectono-stratigraphic units of the Taurides in Afyon area, western Cental Turkey. 5th International Symposium on Eastern Mediteranean Geology, Thessaloniki, Greece, Abstract Book, pp. 80–83.

Gutnic, M., Monod, O., Poisson, A., Dumont, J., 1979. Geologie des Taurides Occidentales (Turquie) Societe Geologique de France Memoir. 137 pp. 1–112.

Hasözbek, A., Satır, M., Erdoğan, B., Akay, E., Siebel, W., 2011. Early Miocene post-collisional magmatism in NW Turkey: geochemical and geochronological constraints. Int. Geol. Rev. 53, 1098–1119.

Hässig, M., Rolland, Y., Sahakyan, L., Sosson, M., Galoyan, G., Avagyan, A., Bosch, D., Müller, C., 2015. Multi-stage metamorphism in the South Armenian Block during the Late Jurassic to Early Cretaceous: tectonics over south-dipping subduction of northern branch of Neotethys. J. Asian Earth Sci. 102, 4–23.

Hatcher Jr., R.D., 2002. Alleghanian (Appalachian) orogeny, a product of zipper tectonics: rotational transpressive continent–continent collision and closing of ancient oceans along irregular margins. In: Martínez Catalán, J.R., Hatcher Jr., R.D., Arenas, R., Díaz García, F. (Eds.), Variscan–Appalachian Dynamics: The Building of the Late Paleozoic Basement. Geological Society of America Special Paper 364, pp. 199–208.

Himmerkus, F., Reischmann, T., Kostopoulos, D., 2009. Triassic rift-related metagranites in the Internal Hellenides, Greece. Geol. Mag. 146 (2), 252–265.

Hoskin, P.W.O., Schaltegger, U., 2003. The composition of zircon and igneous and metamorphic petrogenesis. Rev. Mineral. Geochem. 53, 27–62.

Irvine, T.N., Baragar, W.R.A., 1971. A guide to the chemical classification of the common volcanic rocks. Can. J. Earth Sci. 8, 523–548.

Jolivet, L., Brun, J.P., 2010. Cenozoic geodynamic evolution of the Aegean. Int. J. Earth Sci. 99, 109–138.

Jolivet, L., Lecomte, E., Huet, B., Denèle, Y., Lacombe, O., Labrousse, L., Le Pourhiet, L., Mehl, C., 2010. The north Cycladic detachment system. Earth Planet. Sci. Lett. 289, 87–104.

Keay, S., Lister, G., 2002. African provenance for the metasediments and metaigneous rocks of the Cyclades, Aegean Sea, Greece. Geology 30 (3), 235–238.

Ketin, I., 1966. Türkiyenin tektonik birlikleri. Maden Tetkik ve Arama Genel Müdürlüğü Dergisi 66, 23–34.

Kirkland, C.L., Smithies, R.H., Taylor, R.J.M., Evans, N., McDonald, 2015. Zircon Th/U ratios in magmatic environs. Lithos 212-215, 397–414.

Konak, N., Akdeniz, N., Öztürk, E.M., 1987. Geology of the south of Menderes Massif, I.G.C.P. project no:5, correlation of Variscan and pre-Variscan events of the Alpine Mediterranean mountain belt, field meeting. Mineral Res. Explor. Inst. Turk. 42–53.

Koralay, O.E., Candan, O., Chen, F., Akal, C., Oberhänsli, R., Satır, M., Dora, O.Ö., 2012. Pan-African magmatism in the Menderes Massif: geochronological data from leucocratic tourmaline orthogneisses in western Turkey. Int. J. Earth Sci. 101, 2055–2081.

Kozur, H., 1997. The age of the siliciclastic series (Karareis Formation) of the western Karaburun Peninsula, western Turkey. In: Szaniawski, H. (Ed.)Proceedings of Sixth European Conodont Symposium (ECOS VI)Palaeontologia Polonica 58, pp. 171–189.

Kroner, U., Romer, R.L., 2013. Two plates-many subduction zones: the Variscan orogeny reconsidered. Gondwana Res. 24, 298–329.

Kröner, P.J., O'Brien, A.A., Nemchin, R.T., 2000. Zircon ages for high pressure granulites from south Bohemia, Czech Republic, and their connection to Carboniferous high temperature processes. Contrib. Mineral. Petrol. 138, 127–142.

Kydonakis, K., Kostopoulos, D., Poujol, M., Brun, J.P., Papanikolaou, D., Paquette, J.L., 2014. The dispersal of the Gondwana super-fan system in the eastern Mediterranean: new insights from detrital zircon geochronology. Gondwana Res. 25, 1230–1241.

Le Maitre, R.W., 2002. Igneous rocks-a classification and glossary of terms. Recommendations of the International Union of Geological Sciences Sub Commission on the Systematics of Igneous Rocks, second ed. Cambridge University Press.

Lee, J.K.W., Williams, I.S., Ellis, D.J., 1997. Pb, U and Th diffusion in natural zircon. Nature 390, 159–162.

Linnemann, U., Gerdes, A., Drost, K., Buschmann, B., 2007. The continuum between cadomian orogenesis and opening of the Rheic Ocean: constraints from LA–ICP-MS U–Pb zircon dating and analysis of plate-tectonic setting (Saxo-Thuringian Zone, northeastern Bohemian Massif, Germany). Geol. Soc. Am. Spec. Pap. 423, 61–96.

Linnemann, U., D'Lemos, R., Drost, K., Jeffries, T., Gerdes, A., Romer, R.L., Samson, S.D., Strachan, R.A., Cann, M., 2009. Cadomian tectonics. The Geology of Central Europe Volume 1: Precambrian and Palaeozoic. Geological Society of London, pp. 103–154.

Maniar, P.D., Piccoli, P.M., 1989. Tectonic discrimination of granitoids. Bull. Am. Geogr. Soc. 101, 635–643.

Martin, H., 1993. The mechanisms of petrogenesis of the Archaean continental crust comparison with modern processes. Lithos 30, 373–388.

Mayringer, F., Treloar, P.J., Gerdes, A., Finger, F., Shengelia, D., 2011. New age data from the Dzirula Massif, Georgia: implications for the evolution of the Caucasian Variscides. Am. J. Sci. 311, 404–441.

McCrory, P.A., Wilson, D.S., Stanley, R.G., 2009. Continuing evolution of the Pacific–Juan de Fuca–North America slab window system – a trench–ridge–transform example from the Pacific Rim. Tectonophysics 464, 30–42.

Meinhold, G., Frei, D., 2008. Detrital zircon ages from the islands of Inousses and Psara, Aegean Sea, Greece: constraints on depositional age and provenance. Geol. Mag. 145 (6), 886–891.

Meinhold, G., Reischmann, T., Kostopoulos, D., Lehnert, O., Matukov, D., Sergeev, S., 2008. Provenance of sediments during subduction of Paleo-Tethys: detrital zircon ages and olistolith analysis in Palaeozoic sediments from Chios Island, Greece. Palaeogeogr. Palaeoclimatol. Palaeoecol. 263, 71–91.

Mineral Research and Exploration Institute of Turkey (MTA), 2002,. Geological Map of Turkey, Scale 1:500,000, Ankara.

Moghadam, H.S., Li, X.H., Ling, X.X., Stern, R.J., Santos, J.F., Meinhold, G., Ghorbani, G., Shahabi, S., 2015. Petrogenesis and tectonic implications of Late Carboniferous A-type granites and gabbro-norites in NW Iran: geochronological and geochemical constraints. Lithos 212, 266–279.

Moita, P., Munhá, J., Fonseca, P., Pedro, J., Tassinari, C., Araújo, A., Palácios, T., 2005. Phase equilibria and geochronology of Ossa–Morena eclogites. Acta IV Semana de Geoquímica-8th Congr. Geoquím. Países Língua Portuguesa. 2, pp. 471–474.

Most, T., 2003. Geodynamic Evolution of the Eastern Pelagonian Zone in Northwestern Greece and the Republic of Macedonia. Implications From U/Pb, Rb/Sr, K/Ar, $^{40}Ar/^{39}Ar$ Geochronology and Fission Track Thermochronology (Unpublished PhD. Thesis) Universität Tübingen, Germany (98 pp).

Mposkos, E., Krohe, A., 2004. New evidences of the low-P/high-T pre-Alpine metamorphism and medium-P Alpine overprint of the Pelagonian zone documented in metapelites and orthogneisses from the Voras Massif, Macedonia, northern Greece. Bull. Geol. Soc. Greece 26, 558–567.

Mposkos, E., Kostopoulos, D., Krohe, A., 2001. Low-P/high-T pre-Alpine metamorphism and medium-P Alpine overprint of the Pelagonian zone documented in high-alumina metapelites from the Vernon Massif, western Macedonia, northern Greece. Bull. Geol. Soc. Greece 34 (3), 949–958.

Muttoni, G., Kent, D.V., Garzanti, E., Brack, P., Abrahamsen, N., Gaetani, M., 2003. Early Permian Pangea ‘B’ to Late Permian Pangea ‘A’. Earth Planet. Sci. Lett. 215, 379–394.

Muttoni, G., Gaetani, M., Kent, D.V., 2009. Neotethys opening and the Pangea B to Pangea A transformation during the Permian. GeoArabia 14 (4), 17–48.

Nance, R.D., Gutiérrez-Alonso, G., Keppie, J.D., Linnemann, U., Murphy, J.B., Quesada, C., Strachan, R.A., Woodcock, N.H., 2010. Evolution of the Rheic Ocean. Gondwana Res. 17, 194–222.

Neubauer, F., 2014. Gondwana-land goes Europe. Aust. J. Earth Sci. 107 (1), 147–155.

Nzegge, O.M., Satır, M., Siebel, W., Taubald, H., 2006. Geochemical and isotopic constraints on the genesis of the Late Palaeozoic Deliktaş and Sivrikaya granites from the Kastamonu granitoid belt (Central Pontides, Turkey). Neues Jb. Mineral. Abh. 183, 27–40.

Okay, A.I., 2000. Was the Late Triassic orogeny in Turkey caused by the collision of an oceanic plateau? In: Bozkurt, E., Winchester, J.A., Piper, J.D.A. (Eds.), Tectonics and Magmatism in Turkey and the Surrounding Area. Geological Society, London, Special Publications 173, pp. 25–42

Okay, A.I., 2002. Jadeite-chloritoid-glaucophane-lawsonite blueschists in north-west Turkey: unusually high P/T ratios in continental crust. J. Metamorph. Geol. 20, 757–768.

Okay, A.I., Göncüoğlu, M.C., 2004. The Karakaya complex: a review of data and concepts. Turk. J. Earth Sci. 13, 77–97.

Okay, A.I., Monié, P., 1997. Early Mesozoic subduction in the eastern Mediterranean: evidence from Triassic eclogite in northwest Turkey. Geology 25, 595–598.

Okay, A.I., Nikishin, A.M., 2015. Tectonic evolution of the southern margin of Laurasia in the Black Sea region. Int. Geol. Rev. http://dx.doi.org/10.1080/00206814.2015.1010609.

Okay, A.I., Tüysüz, O., 1999. Tethyan sutures of northern Turkey. In: Durand, B., Jolivet, L., Horváth, F., Séranne, M. (Eds.), The Mediterranean Basins: Tertiary Extension Within the Alpine Orogen. Geological Society, London, Special Publications 156, pp. 475–515.

Okay, A.I., Tansel, I., Tüysüz, O., 2001. Obduction, subduction and collusion as reflected in the Upper Cretaceous–Lower Eocene sedimentary record of western Turkey. Geol. Mag. 138 (2), 117–142.

Okay, A.I., Monod, O., Monie, P., 2002. Triassic blueschists and eclogites from northwest Turkey: vestiges of the Paleo-Tethyan subduction. Lithos 64, 155–178.

Okay, A.I., Satır, M., Siebel, W., 2006. Pre-Alpide orogenic events in the eastern Mediterranean region. In: Gee, D.G., Stephenson, R.A. (Eds.), European Lithosphere Dynamics. Geological Society of London, Memoirs 32, pp. 389–405.

Okay, A.I., Satir, M., Zattin, M., Cavazza, W., Topuz, G., 2008. An Oligocene ductile strike-slip shear zone: Uludağ Massif, northwest Turkey – implications for the escape tectonics. Geol. Soc. Am. Bull. 120, 893–911.

Okay, A.I., Altıner, D., Kılıç, A.M., 2014a. Triassic limestone, turbidites and serpentinite–the Cimmeride orogeny in the central Pontides. Geol. Mag. http://dx.doi.org/10.1017/S0016756814000429.

Okay, A.I., Sunal, G., Tüysüz, O., Sherlock, S., Keskin, M., Kylander-Clark, A.R.C., 2014b. Low-pressure-high-temperature metamorphism during extension in a Jurassic magmatic arc, central Pontides, Turkey. J. Metamorph. Geol. 32, 49–69.

Okrusch, M., Bröcker, M., 1990. Eclogites associated with high-grade blueschists in the Cyclades archipelago, Greece: a review. Eur. J. Mineral. 2, 451–478.

Özcan, A., Göncüoğlu, C.M., Turhan, N., Uysal, S., Şentürk, K., 1988. Late Paleozoic evolution of the Kütahya-Bolkardağ Belt. METU J. Pure Appl. Sci. 21, 211–220.

Özdamar, Ş., Billor, M.Z., Sunal, G., Esenli, F., Roden, M.F., 2013. First U–Pb SHRIMP zircon and ^{40}Ar/^{39}Ar ages of metarhyolites from the Afyon–Bolkardag Zone, SW Turkey: implications for the rifting and closure of the Neo-Tethys. Gondwana Res. 24, 377–391.

Özer, S., Özgen, İ.Ö., 2012. Correlation of the Upper Cretaceous sequences between Afyon Zone and Menderes massif based on the new palaeontological data (rudist and planktic foraminifer). 65th Geological Congress of Turkey, pp. 438–439.

Özgül, N., 1976. Some geological aspects of the Taurits orogenic belt (Turkey). Bull. Geol. Soc. Turk. 19, 65–78 (in Turkish with English abstract).

Özgül, N., 1984. In: Tekeli, O., Göncüoğlu, M.C. (Eds.), Stratigraphy and tectonics evolution of the central Taurides. Geology of the Taurus Belt. Proceedings of the International Tauride Symposium, Mineral Research and Exploration Institute of Turkey (MTA) Publication, pp. 77–90.

Özgül, N., 1997. Stratigraphy of the tectono-stratigraphic units in the region Bozkır-Hadim-Taşkent (northern central Taurides). Bull. Mineral Res. Explor. Turk. 119, 113–174 (in Turkish with English abstract).

Papanikolaou, D., 2013. Tectonostratigraphic models of the Alpine terranes and subduction history of the Hellenides. Tectonophysics 595–596, 1–24.

Pearce, J.A., 1983. Role of the sub-continental lithosphere in magma genesis at active continental margins. In: Hawkesworth, C.J., Norry, M.J. (Eds.), Continental Basalts and Mantle Xenoliths. Shiva, Nantwich, pp. 230–249.

Pearce, J.A., 1996. Source and settings of granitic rocks. Episodes 19 (4), 120–125.

Pearce, J.A., Harris, N.B.W., Tindle, A.G., 1984. Trace element discrimination diagrams for the tectonic interpretation of granitic rocks. J. Petrol. 25, 956–983.

Philippon, M., Brun, J.P., Gueydan, F., 2012. Deciphering subduction from exhumation in the segmented Cycladic Blueschist Unit (Central Aegean, Greece). Tectonophysics 524-525, 116–134.

Pourteau, A., Sudo, O., Candan, O., Lanari, P., Vidal, O., Oberhänsli, R., 2013. Neotethys closure history of Anatolia: insights from ^{40}Ar-^{39}Ar geochronology and P-T estimation in high-pressure metasedimentary rocks. J. Metamorph. Geol. 31, 585–606.

Qian, Q., Hermann, J., 2013. Partial melting of lower crust at 10–15 kbar, constraints on adakite and TTG formation. Contrib. Mineral. Petrol. 65, 1195–1224.

Reischmann, T., 1998. Pre-alpine origin of tectonic units from the metamorphic complex of Naxos, Greece, identified by single zircon Pb/Pb dating. Bull. Geol. Soc. Greece 32 (3), 101–111.

Reischmann, T., Kostopoulos, D.K., Loos, S., Anders, B., Avgerinas, A., Sklavounos, S.A., 2001. Late Paleozoic magmatism in the basement rocks southwest of the Mt. Olympos, Central Pelagonian Zone, Greece: remnants of a Permo-Carboniferous magmatic arc. Bull. Geol. Soc. Greece 25, 985–993.

Ring, U., Gessner, K., Passchier, C.W., Güngör, T., 1999. The Menderes Massif of western Turkey and the Cycladic Massif in the Aegean – do they really correlate. J. Geol. Soc. Lond. 156, 3–6.

Robertson, A.H.F., 2006. Sedimentary evidence from the south Mediterranean region (Sicily, Crete, Peloponnese, Evia) used to test alternative models for the regional tectonic setting of Tethys during Late Palaeozoic-Early Mesozoic time. In: Robertson, A.H.F., Mountrakis, D. (Eds.), Tectonic Development of the Eastern Mediterranean Region. Geological Society, London, Special Publications 260, pp. 91–154.

Robertson, A.H.F., Dixon, J.E., 1984. Introduction: aspects of the geological evolution of the eastern Mediterranean. In: Dixon, J.E., Robertson, A.H.F. (Eds.), The Geological Evolution of the Eastern Mediterranean. Geological Society, London, Special Publications 17, pp. 1–74.

Robertson, A.H.F., Pickett, E.A., 2000. Palaeozoic–Early Tertiary Tethyan evolution of mélanges, Rift and passive margin units in the Karaburun Peninsula (western Turkey) and Chios Island (Greece). In: Bozkurt, E., Winchester, J.A., Piper, J.D.A. (Eds.), Tectonic and Magmatism in Turkey and the Surrounding Area. Geological Society, London, Special Publications 173, pp. 43–82.

Robertson, A.H.F., Ustaömer, T., 2009a. Upper Palaeozoic subduction/accretion processes in the closure of Palaeotethys: evidence from the Chios Melange (E Greece), the Karaburun Melange (W Turkey) and the Teke Dere Unit (SW Turkey). Sediment. Geol. 220, 29–59.

Robertson, A.H.F., Ustaömer, T., 2009b. Formation of the late Palaeozoic Konya complex and comparable units in southern Turkey by subduction–accretion processes: implications for the tectonic development of Tethys in the eastern Mediterranean region. Tectonophysics 473, 113–148.

Robertson, A.H.F., Ustaömer, T., 2011. Role of tectonic-sedimentary mélange and Permian–Triassic cover units, central southern Turkey in Tethyan continental margin evolution. J. Asian Earth Sci. 40, 98–120.

Robertson, A.H.F., Dixon, J.E., Brown, S., Collins, A., Morris, A., Pickett, E., Sharp, I., 1996. Alternative tectonic models for the Late Palaeozoic–Early Tertiary development of Tethys in the eastern Mediterranean region. In: Morris, A., Tarling, D.H. (Eds.), Palaeomagnetism and Tectonics of the Mediterranean Region. Geological Society, London, Special Publications 105, pp. 239–263.

Roger, F., Matte, P., 2005. Early Variscan HP metamorphism in the western Iberian Allochthon-A 390 Ma U–Pb age for the Braganca eclogite (NW Portugal). Int. J. Earth Sci. 94, 173–179.

Rolland, Y., Sosson, M., Adamia, S., Sadradze, N., 2011. Prolonged Variscan to Alpine history of an active Eurasian margin (Georgia, Armenia) revealed by ^{40}Ar/^{39}Ar dating. Gondwana Res. 20, 798–815.

Romano, S.S., Brix, M.R., Dorr, W., Fiala, J., Krenn, E., Zulauf, G., 2006. The Carboniferous to Jurassic evolution of the pre-Alpine basement of Crete: constraints from U-Pb and U-(Th)-Pb dating of orthogneiss, fission-track dating of zircon, structural and petrological data. In: Robertson, A.H.F., Mountrakis, D. (Eds.), Tectonic Development of the Eastern Mediterranean Region. Geological Society, London, Special Publications 260, pp. 69–90.

Rötzler, J., Romer, R.L., 2001. P–T–t evolution of ultrahigh-temperature granulites from the Saxon Granulite Massif, Germany. Part I: petrology. J. Petrol. 42, 1995–2013.

Rubatto, D., 2002. Zircon trace element geochemistry: partitioning with garnet and the link between U–Pb ages and metamorphism. Chem. Geol. 184, 123–138.

Saccani, E., Azimzadeh, Z., Dilek, Y., Jahangiri, A., 2013. Geochronology and petrology of the Early Carboniferous Misho Mafic Complex (NW Iran), and implications for the melt evolution of Paleo-Tethyan rifting in western Cimmeria. Lithos 162, 264–278.

Saunders, A.D., Tarney, J., 1980. The geochemistry of basalts from a back arc spreading centre in the east Scotia Sea. Geochim. Cosmochim. Acta 43, 555–572.

Schenker, F.L., Burg, J.-P., Kostopoulos, D., Moulas, E., Larionov, A., von Quadt, A., 2014. From Mesoproterozoic magmatism to collisional Cretaceous anatexis: tectonomagmatic history of the Pelagonian Zone, Greece. Tectonics 33, 1552–1576.

Şen, C., 2007. Jurassic volcanism in the eastern Pontides: is it rift related or subduction related? Turk. J. Earth Sci. 16, 523–539.

Şengör, A.M.C., 1979. Mid-Mesozoic closure of Permo-Triassic Tethys and its implications. Nature 279, 590–593.

Şengör, A.M.C., Yılmaz, Y., 1981. Tethyan evolution of Turkey: a plate tectonic approach. Tectonophysics 75, 181–241.

Şengör, A.M.C., Yılmaz, Y., Ketin, I., 1980. Remnants of a pre-late Jurassic ocean in northern Turkey: fragments of Permian-Triassic Paleo-Tethys. Geol. Soc. Am. Bull. 91, 499–609.

Şengör, A.M.C., Yilmaz, Y., Sungurlu, O., 1984. Tectonics of the Mediterranean Cimmerides: nature and evolution of the western termination of Palaeo-Tethys. In: Dixon, J.E., Robertson, A.H.F. (Eds.), The Geological Evolution of the Eastern Mediterranean. Geological Society, London, Special Publications 17, pp. 77–112.

Sherlock, S., Kelley, S.P., Inger, S., Harris, N., Okay, A.I., 1999. ^{40}Ar-^{39}Ar and Rb-Sr geochronology of high-pressure metamorphism and exhumation history of the Tavşanlı Zone, NW Turkey. Contrib. Mineral. Petrol. 137, 46–58.

Stampfli, G., 2000. Tethyan oceans. In: Bozkurt, E., Winchester, J.A., Piper, J.D.A. (Eds.), Tectonics and Magmatism in Turkey and the Surrounding Area. Geological Society, London, Special Publications 173, pp. 1–23.

Stampfli, G.M., Borel, G.D., 2002. A plate tectonic model for the Paleozoic and Mesozoic constrained by dynamic plate boundaries and restored synthetic oceanic isochrons. Earth Planet. Sci. Lett. 196, 17–33.

Stampfli, G.M., Kozur, H., 2006. Europe from the Variscan to the Alpine cycles. In: Gee, D.G., Stephenson, R. (Eds.). European Lithosphere Dynamics: Geological Society, London, Memoir 32, 57–82.

Stampfli, G., Mosar, J., Faure, P., Pillevuit, A., Vannay, J.C., 2001. Permo-Mesozoic evolution of the western Tethys real: the Neotethys East Mediterranean basin connection. In: Ziegler, P., Cavazza, W., Robertson, A.H.F., Crasquin-Soleau, S. (Eds.), Peri-Tethys Memoir No. 5 Peri-Tethyan Rift/Wrench Basins and Passive Margins. Museum National d'Histoire Naturelle, Memoirs, pp. 51–108.

Stampfli, G.M., von Raumer, J., Borel, G.D., 2002. The Paleozoic evolution of pre-Variscan terranes: from peri-Gondwana to the Variscan collision. In: Martinez-Catalan, J.R., Hatcher, R.D., Arenas, R., Diaz Garcia, F. (Eds.), Variscan Appalachian Dynamics: The Building of the Upper Paleozoic Basement. Geological Society of America Special Paper 364, pp. 263–280.

Stampfli, G.M., Vavassis, I., De Bono, A., Rosselet, F., Matti, B., Bellini, M., 2003. Remnants of the Paleotethys oceanic suture-zone in the western Tethyan area. In: Cassinis, G., Decandia, F.A. (Eds.), Stratigraphic and Structural Evolution on the Late Carboniferous to Triassic Continental and Marine Successions in Tuscany (Italy): Regional Reports and General Correlation. Bolletino della Società Geologica Italiana, Volume Speciale 2, pp. 1–24.

Stampfli, G.M., Hochard, C., Vérard, C., Wilhem, C., von Raumer, J., 2013. The formation of Pangea. Tectonophysics 593, 1–19.

Stosch, H., Lugmair, G., 1990. Geochemistry and evolution of MORB-type eclogites from the Münchberg Massif, southern Germany. Earth Planet. Sci. Lett. 99, 230–249.

Sun, S.S., McDonough, W.F., 1989. Chemical and isotopic systematics of ocean basalts: implications for mantle composition and processes. In: Saunders, A.D., Norry, M.J. (Eds.),

Magmatism in Ocean Basins. Geological Society, London, Special Publications 42, pp. 313–345.
Topuz, G., Altherr, R., Kalt, A., Satır, M., Werner, O., Schwartz, W.H., 2004. Aluminous granulites from the Pulur Complex, NE Turkey: a case of partial melting, efficient melt extraction and crystallization. Lithos 72, 183–207.
Topuz, G., Altherr, R., Schwarz, W.H., Dokuz, A., Meyer, H.P., 2007. Variscan amphibolite facies rocks from the Kurtoğlu metamorphic complex, Gümüşhane area, eastern Pontides Turkey. Int. J. Earth Sci. 96, 861–873.
Topuz, G., Altherr, R., Siebel, W., Schwarz, W.H., Zack, T., Hasözbek, A., Barth, M., Satır, M., Şen, C., 2010. Carboniferous high-potassium I-type granitoid magmatism in the eastern Pontides: the Gümüşhane pluton (NE Turkey). Lithos 116, 92–110.
Topuz, G., Göçmengil, G., Rolland, Y., Çelik, Ö.F., Zack, T., Schmitt, A.K., 2013. Jurassic accretionary complex and ophiolite from northeast Turkey: no evidence for the Cimmerian continental ribbon. Geology 41, 255–258.
Torsvik, T.H., Cocks, L.R.M., 2013. Gondwana from top to base in space and time. Gondwana Res. 24, 999–1030.
Ustaömer, T., Robertson, A.H.F., 1993. Late Palaeozoic-Early Mesozoic marginal basins along the active southern continental margin of Eurasia: evidence from the central Pontides (Turkey) and adjacent regions. Geol. J. 28, 219–238.
Ustaömer, P.A., Ustaömer, T., Robertson, A.H.F., 2012a. Ion probe U–Pb dating of the central Sakarya basement: a peri-Gondwana terrane intruded by late Lower Carboniferous subduction/collision related granitic rocks. Turk. J. Earth Sci. 21, 905–932.
Ustaömer, T., Robertson, A.H.F., Ustaömer, P.A., Gerdes, A., Peytcheva, I., 2012b. Constraints on Variscan and Cimmerian magmatism and metamorphism in the Pontides (Yusufeli–Artvin area), NE Turkey from U–Pb dating and granite geochemistry. In: Robertson, A.H.F., Parlak, O., Ünlügenç, U.C. (Eds.), Geological Development of Anatolia and the Easternmost Mediterranean Region. Geological Society, London, Special Publications (doi:10.1144/SP372.13).
Vavassis, I., De Bono, A., Valloton, A., Stampfli, G.M., Amelin, Y., 2000. U-Pb and Ar-Ar geochronological data from Pelagonia basement in Evia (Greece): geodynamic implications for the Paleotethys subduction. Schweiz. Mineral. Petrogr. Mitt. 80, 21–43.
Veevers, J.J., 2004. Gondwanaland from 650–500 Ma assembly through 320 Ma merger in Pangea to 185–100 Ma breakup: supercontinental tectonics via stratigraphy and radiometric dating. Earth Sci. Rev. 68, 1–132.
von Raumer, J.F., Stampfli, G.M., 2008. The birth of the Rheic Ocean-Early Palaeozoic subsidence patterns and subsequent tectonic plate scenarios. Tectonophysics 461, 9–20.
von Raumer, J.F., Bussy, F., Schaltegger, U., Schulz, B., Stampfli, G.M., 2013. Pre-Mesozoic Alpine basements-their place in the European Paleozoic framework. Geol. Soc. Am. Bull. 125, 89–108.
Wilson, M., 1989. Igneous Petrogenesis. Chapman and Hall, London, p. 466.
Xypolias, P., Dörr, W., Zulauf, G., 2006. Late Carboniferous plutonism within the pre-Alpine basement of the external Hellenides (Kithira, Greece): evidence from U-Pb zircon dating. J. Geol. Soc. Lond. 163, 539–547.
Yılmaz, O., Boztuğ, D., 1986. Kastamonu granitoid belt of northern Turkey: first arc plutonism product related to the subduction of the Paleo-Tethys. Geology 14, 179–183.
Yılmaz, Y., Tüysüz, O., Yiğitbaş, E., Genç, Ş.C., Şengör, A.M.C., 1997. Geology and tectonic evolution of the Pontides. In: Robinson, A.G. (Ed.), Regional and Petroleum Geology of the Black Sea and Surrounding Region 68. AAPG Memoir, pp. 183–226.
Zanchi, A., Garzanti, E., Larghi, C., Gaetani, M., 2003. The Variscan orogeny in Chios (Greece): Carboniferous accretion along a Palaeotethyan active margin. Terra Nova 15, 213–223.
Zhang, H.F., Zhu, R.X., Santosh, M., Ying, J.F., Su, B.X., Hu, Y., 2013. Episodic widespread magma underplating beneath the North China Craton in the Phanerozoic: implications for craton destruction. Gondwana Res. 23, 95–107.
Zulauf, G., Romano, S.S., Dörr, W., Fiala, J., 2007. Crete and the Minoan terranes: age constraints from U-Pb dating of detrital zircons. In: Linnemann, U., Nance, R.D., Kraft, P., Zulauf, G. (Eds.), The Evolution of the Rheic Ocean: From Avalonian–Cadomian Active Margin to Alleghenian–Variscan Collision. Geological Society of America Special Paper 423, pp. 401–411.